Ion–laser interactions: The most complete solution

Héctor Moya-Cessa [a,*], Francisco Soto-Eguibar [a], José M. Vargas-Martínez [a],
Raúl Juárez-Amaro [b], Arturo Zúñiga-Segundo [c]

[a] *INAOE, Coordinación de Optica, Apdo. Postal 51 y 216, 72000 Puebla, Pue., Mexico*
[b] *Universidad Tecnológica de la Mixteca, Apdo. Postal 71, Huajuapan de León, Oax., 69000, Mexico*
[c] *Departamento de Física, Escuela Superior de Física y Matemáticas Edificio 9, Unidad Profesional 'Adolfo López Mateos', 07738 México, DF, Mexico*

ARTICLE INFO

ABSTRACT

Trapped ions are considered one of the best candidates to perform quantum information processing. By interacting them with laser beams they are, somehow, easy to manipulate, which makes them an excellent choice for the production of nonclassical states of their vibrational motion, the reconstruction of quasiprobability distribution functions, the production of quantum gates, etc. However, most of these effects have been produced in the so-called low intensity regime, this is, when the Rabi frequency (laser intensity) is much smaller than the trap frequency. Because of the possibility to produce faster quantum gates in other regimes it is of importance to study this system in a more complete manner, which is the motivation for this contribution. We start by studying the way ions are trapped in Paul traps and review the basic mechanisms of trapping. Then we show how the problem may be completely solved for trapping states; i.e., we find (exact) eigenstates of the full Hamiltonian. We show how, in the low intensity regime, Jaynes–Cummings and anti-Jaynes–Cummings interactions may be obtained, without using the rotating wave approximation and analyze the medium and high intensity regimes where dispersive Hamiltonians are produced. The traditional approach (low intensity regime) is also studied and used for the generation of non-classical states of the vibrational wavefunction. In particular, we show how to add and subtract vibrational quanta to an initial state, how to produce specific superpositions of number states and how to generate NOON states for the two-dimensional vibration of the ion. It is also shown how squeezing may be measured. The time dependent problem is studied by using Lewis–Ermakov methods. We give a solution to the problem when the time dependence of the trap is considered and also analyze a specific (artificial) time dependence that produces squeezing of the initial vibrational wave function. A way to mimic the ion–laser interaction via classical optics is also introduced.

© 2012 Elsevier B.V. All rights reserved.

Contents

* Corresponding author. Fax: +52 222 2472940.
  E-mail address: moyah@ictp.it (H. Moya-Cessa).

1. Introduction

The possibility to trap small clouds of particles, or inclusive to trap individual atoms or ions, in a small region of space, was opened with the invention of electromagnetic traps. These traps allow to study isolated particles for long periods of time. The Kingdon trap [1] is considered the first type of trap developed. It consists of a metallic filament surrounded by a metallic cylinder, and a direct current voltage applied between them; the ions are attracted by the filament, but its angular momentum makes them turn around in circular orbits, with a low probability to crash against it. A dynamic version of this trap can be obtained if an alternate current voltage is applied between the poles. However, this type of trap was not widely used at that time, because it has short storage times and because its potential is not harmonic. In 1936, Penning invented another trap [2] in which the action of magnetic fields together with electric fields make possible the trapping of ions. The complete development of this type of trap was reached when, in 1959, Wolfgang Paul designed an electrodynamic trap (now called Paul trap) [3]. In the Paul trap the idea is that a charged particle cannot be confined in a region of space by constant electric fields, instead an electric field oscillating at radio frequency, must be applied. The Paul trap uses not only the focusing or defocusing forces of the quadrupolar electric field acting on the ions, but also takes advantage of the stability properties of the equations of motion. The ions trapped individually are very interesting, mainly because they are simple systems to be studied. In particular, we take advantage that the ion motion in the Paul trap is approximately harmonic, making this system a simple one, allowing a better and more direct comparison with the theory. Individual ions of Ca+, Be+, Ba+ and Mg+, can be stored, even for several days. The trapped ions can be used to implement quantum gates, and a bunch of ions arranged in a chain, is a promising tool to achieve a quantum computer (each ion in the chain is a fundamental unit of information or qubit) [4]. The trapping of individual ions also offers a lot of possibilities in spectroscopy [5], in the research of frequency standards [6,7], in the study of quantum jumps [8], the engineering of specific Hamiltonians [9] and in the generation of nonclassical vibrational states of the ion [10–17], to name some. To make the ions more stable in the trap, increasing the time of confinement, and also to avoid undesirable random motions, it is required that the ion be in its vibrational ground state. This can be accomplished by means of an adequate use of lasers; with the help of these lasers, the internal energy levels of the trapped ion can be coupled to their vibrational quantum states, in such a way, that for a certain detuning, the coupling is equivalent to the Jaynes–Cummings Hamiltonian [18–23]. On the other hand, the beam that induces the coupling can be tuned to allow interactions that generate simultaneous transitions of the internal and vibrational states, either to lower vibrational energy levels (while passing from the excited to the ground state) or to higher vibrational energy levels (while passing from the ground to the excited state); this type of coupling is called anti-Jaynes–Cummings. Alternating successively Jaynes–Cummings and anti-Jaynes–Cummings interactions, the trapped ion can be driven to its vibrational ground state. In this paper, we study part of the physics of the trapped ions interacting with a laser field. By using a set of time-dependent unitary transformations, it is shown that this system is equivalent to the interaction between a quantized field and a two level system with time dependent parameters. The Hamiltonian is linearized in such a way that it can be solved with methods that are found in the literature, and that involve time-dependent parameters. The linearization is free of approximations and assumptions on the parameters of the system as are; for instance, the Lamb-Dicke parameter, the time-dependency of the trap frequency and the detuning. Thus, we can obtain the best solution for this kind of systems. Also, we analyze a particular case of time-dependency of the trap frequency.

Because we will assume an ion trapped in a Paul trap, in Section 2, we review the basic mechanisms of it. In Section 3, we show how exact eigenstates may be obtained for the ion–laser system. In Section 4, we show how this interaction may be solved in different regimes. In Section 5, the standard approach to this interaction is treated; i.e., the low intensity regime, where by application of the rotating wave approximation, Jaynes–Cummings and anti-Jaynes–Cummings interactions may be generated. By using this approach, we show how nonclassical states may be generated; in particular, we show how to add phonons to a vibrational state, how to filter specific superpositions of the motional wave function and how to generate NOON states in ions vibrating in two dimensions. We also propose here a scheme that allows the measurement of squeezing. In Section 6, we analyze the case of an ion with a time-dependent frequency interacting with a laser beam. By doing a series of unitary transformations, we linearize the Hamiltonian of the system to an exact soluble form; this linearization is also valid for any detuning and for any time dependence of the trap. In Section 7, we show how the ion–laser interaction may be modeled by evanescently coupling waveguides and Section 8 is left for conclusions.

2. Paul trap

2.1. The quadrupolar potential of the trap

As we already said, the Paul trap uses static and oscillating electric potentials to confine charged particles. A charged particle is linked to an axis if a linear restoring force acts over it; i.e., if the force is

$$\vec{F} = -c\vec{r}, \tag{1}$$

where $\vec{r}$ is the particle position and c is a constant. In other words, if the particle moves under the action of a parabolic potential, that it can be written in the general form as

$$\Phi(x, y, z) = A(\alpha x^2 + \beta y^2 + \gamma z^2), \tag{2}$$

where A is another constant. The potential Φ must satisfy the Laplace equation, which means that

$$\nabla^2 \Phi = 0, \tag{3}$$

where ∇^2 is the Laplacian operator. The Laplace equation (3) imposes the condition

$$\alpha + \beta + \gamma = 0. \tag{4}$$

To satisfy the above condition, we have several possibilities.
(a) We make $\alpha = 1$, $\beta = 0$ and $\gamma = -1$, and this takes us to the bidimensional potential

$$\Phi = \frac{\Phi_0}{2r_0^2}(x^2 - z^2). \tag{5}$$

(b) Another possibility is $\alpha = 1$, $\beta = 1$ and $\gamma = -2$, and in this case we have, in cylindrical coordinates, the potential

$$\Phi = \frac{\Phi_0}{r_0^2 + 2z_0^2}(r^2 - 2z^2), \tag{6}$$

with $r_0^2 = 2z_0^2$.

Configuration (a), Eq. (5), is created by four hyperbolic electrodes linearly extended in the z direction, as shown in Fig. 1. Configuration (b), expression (6), is created by two electrodes in the form of a hyperboloid of revolution around the z axis.

The most used trap is the linear trap, as the one shown in Fig. 1, but with poles having circular transverse section instead of hyperbolic, because it is easier to build. This cylindrical form does not correspond to some set of values of (4), but numerically it has been demonstrated that the potential produced by these electrodes near the axis of the trap is very similar to the one produced by the hyperbolic electrodes [24].

For the tridimensional case the magnitude of the field is given by

$$E_x = \frac{\Phi_0}{r_0^2}x, \qquad E_y = \frac{\Phi_0}{r_0^2}y, \qquad E_z = 2\frac{\Phi_0}{r_0^2}z. \tag{7}$$

Expressions (6) and (7) reveal that the components r and z of the electric field are independent from each other, and that they are linear functions of r and z, respectively. We also see that we have a harmonic oscillator potential (parabolic and attractive) in the radial direction and a parabolic repulsive potential in the z direction. If a constant voltage Φ_0 is applied, and an ion is injected, the ion will oscillate harmonically in the x–y plane, but because of the opposite sign in the field E_z, its amplitude in the z direction will grow exponentially. The particles will be out of focus, and they will be lost by crashing against the electrodes. Thus, the quadrupolar static potential, by itself, is not capable to confine the particles in three dimensions; at most, with this potential, we get unstable equilibrium. We will see next, how to solve this problem.
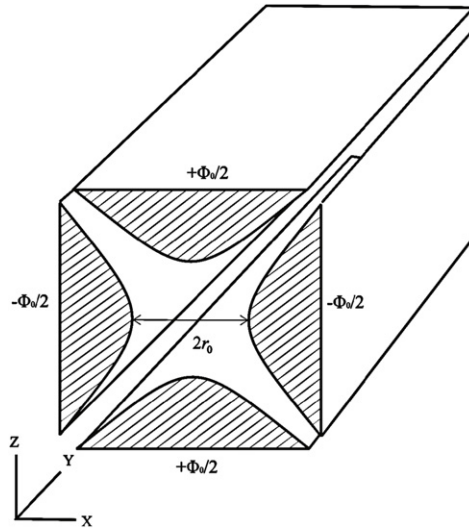
Fig. 1. Electrode structure for the bidimensional configuration expressed by Eq. (5).
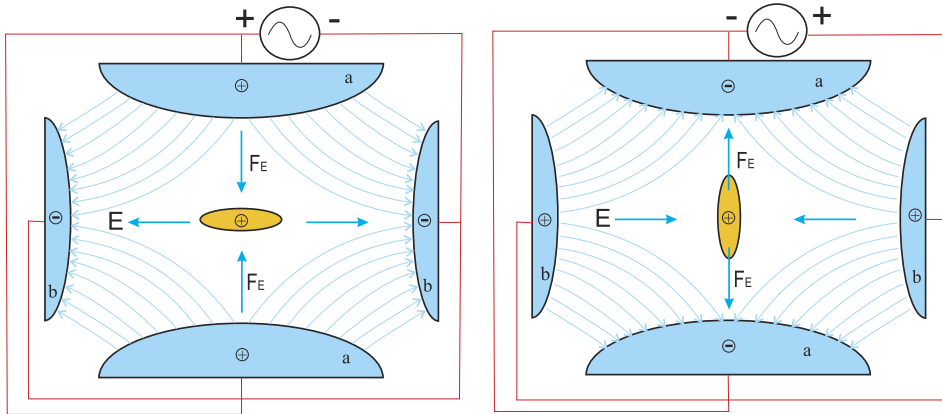
Fig. 2. Scheme of a Paul trap to store charged particles using oscillating electric fields generated by a quadrupole. The figure shows two states during an alternate current cycle.

2.2. Oscillating potential of the trap

To avoid the unstable behavior of the charged particles under a static potential, the trap must be modified. If an oscillatory electric field is applied, the particles can be confined. Because of the periodic change of the sign of the electric force, we get focusing and defocusing in both directions of r and z alternatively with time.

If the applied voltage is given by a continuous voltage plus a voltage with a frequency Ω, we have

$$\Phi_0 = U_0 + V_0 \cos \Omega t, \tag{8}$$

and the potential in the axis of the trap is

$$\Phi = \frac{U_0 + V_0 \cos \Omega t}{r_0^2 + 2z_0^2}(r^2 - 2z^2), \tag{9}$$

where r_0 is the distance from the trap center to the electrode surface.

In Fig. 2, we show a transversal section of a Paul trap using an oscillating electric field.

2.3. Motion in the Paul trap

We will study now some details of the ion motion in a Paul trap. Let us consider the particular case of just one ion, in three dimensions. If m is the mass of the ion, and e its charge, the equation of motion is

$$m\ddot{\vec{r}}(x, y, z) = q\vec{E} = -q\nabla\Phi. \tag{10}$$

In order to analyze the trapping conditions, we explicitly write each component as

$$\ddot{x} = -\frac{2e}{mR^2}(U_0 + V_0 \cos \Omega t)x, \tag{11}$$

$$\ddot{y} = -\frac{2e}{mR^2}(U_0 + V_0 \cos \Omega t)y, \tag{12}$$

and

$$\ddot{z} = \frac{2e}{mR^2}2(U_0 + V_0 \cos \Omega t)z, \tag{13}$$

where $R^2 = r_0^2 + 2z_0^2$.

Making the substitution

$$a_r = \frac{8eU_0}{mR^2\Omega^2} = -\frac{a_z}{2}, \qquad q_r = -\frac{4eV_0}{mR^2\Omega^2} = -\frac{q_z}{2}, \qquad \tau = \frac{\Omega t}{2}, \tag{14}$$

Eqs. (11)–(13) take the form of the Mathieu equation; i.e., take the form

$$\frac{d^2x}{d\tau^2} + (a_r - 2q_r \cos 2\tau)x = 0, \tag{15}$$

$$\frac{d^2y}{d\tau^2} + (a_r - 2q_r \cos 2\tau)y = 0, \tag{16}$$

and

$$\frac{d^2z}{d\tau^2} + (a_z - 2q_z \cos 2\tau)z = 0, \tag{17}$$

respectively. We can write the three equations as the following one,

$$\frac{d^2u_i}{d\tau^2} + (a_i - 2q_i \cos 2\tau)u_i = 0. \tag{18}$$

The subindices $i = r, z$ corresponds to the quantities associated with the axial and radial motions of the ion, respectively. The quantities u_i represent the displacement in the directions r and z.

2.4. Approximated solution to the Mathieu equation

The Mathieu equation is a linear ordinary differential equation with periodic coefficients. This equation can be solved using Floquet's theorem [25], which takes us to the general solution

$$u_i(\tau) = A_i e^{i\beta_i\tau}\phi(\tau) + B_i e^{-i\beta_i\tau}\phi(-\tau), \tag{19}$$

where A_i, B_i and β_i are constants determined by the initial position, by the initial velocity of the ion, and by the trap parameters a and q, and

$$\phi(\tau) = \phi(\tau + \pi) = \sum_{n=-\infty}^{+\infty} C_n e^{2in\tau} \tag{20}$$

is a periodic function.

The Mathieu equation has two types of solutions.

(1) Stable motion. When the characteristic exponent β is real, the variable $u(\tau)$ is bounded, and in consequence the motion is stable. That means that the particle oscillates with bounded amplitudes and without crashing against the electrodes. These conditions allow to trap the ion.

(2) Unstable motion. When the characteristic exponent β has an imaginary part, the function $u(\tau)$ has an exponential growing contribution. The amplitudes grow exponentially and the particles are lost when they crash against the electrodes. The boundaries of the stability regions correspond to zero and integer values of β_i, and the first region of stability is surrounded by the four lines $\beta_r = 0$, $\beta_r = 1$, $\beta_z = 0$, and $\beta_z = 1$, as shown in Fig. 3 [26].

As β_i is determined by a and q, the Mathieu equation has stable solutions as a function of a and q. Stability regions for the solutions of Eq. (18) correspond to regions in the space of the parameters $a - q$, where there is an overlap of the stability regions in the axial and radial directions.
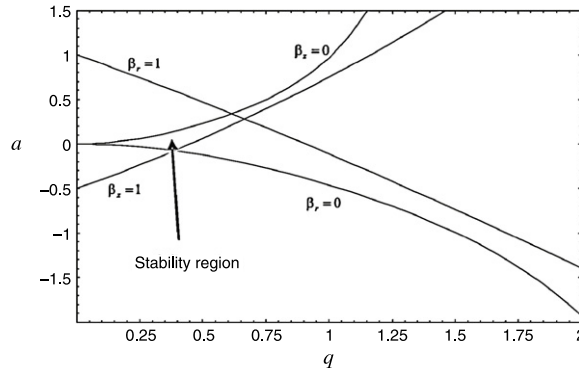
Fig. 3. Stability region in the Paul trap.

In the literature it is not possible to find analytic solutions for Eq. (18), but in most of the applications a specification of the map of stability of the solutions is enough, and a detailed functional dependence is not necessary. However, an approximated solution can be given in the stability region of interest. To this end, we can write expression (19) as

$$u_i(\tau) = A_i \sum_{n=-\infty}^{+\infty} C_{2n}^i \cos(2n + \beta_i)\tau + B_i \sum_{n=-\infty}^{+\infty} C_{2n}^i \sin(2n + \beta_i)\tau \qquad (21)$$

where, as we already said, A_i and B_i are determined by the initial position $u_i(0)$ and initial speed $\dot{u}_i(0)$ of the ion, respectively. The subindices $i = r, z$ coincide with the quantities associated with the radial and axial ion motion, respectively.

The coefficients in the solution (21) are given by the recurrence relations

$$C_{2n+2}^i - D_{2n}^i C_{2n}^i + C_{2n-2}^i = 0, \qquad (22)$$

with

$$D_{2n}^i = \frac{a_i - (2n + \beta_i)^2}{q_i}. \qquad (23)$$

Once given a_i and q_i, the quantities C_{2n}^i and β_i can be calculated. If we define,

$$G_{2n}^i = \frac{C_{2n}^i}{C_0^i}, \qquad A_i' = A_i C_0^i, \qquad B_i' = B_i C_0^i, \qquad (24)$$

and we make

$$u_i(t) = u_i^s(t) + u_i^m(t), \qquad (25)$$

we get, from Eq. (21),

$$u_i^s(\tau) = A_i' \cos \omega_i t + B_i' \sin \omega_i t, \qquad (26)$$

and

$$u_i^m(\tau) = \sum_{n=1}^{\infty} (A_i' \cos \omega_i t + B_i' \sin \omega_i t)(G_{2n}^i + G_{-2n}^i) \cos n\Omega t + (B_i' \cos \omega_i t - A_i' \sin \omega_i t)(G_{2n}^i - G_{-2n}^i) \sin n\Omega t, \qquad (27)$$

where $\omega_i = \beta_i \Omega/2$.

Analyzing Eqs. (26) and (27), it is possible to realize that the ion motion has two components: $u_i^s(t)$, a harmonic oscillation of frequency ω_i, and, $u_i^m(t)$, a superposition of several harmonics with a fundamental frequency Ω, and amplitudes modulated by the frequency ω_i. However, the proportion of the two components, the values of ω_i, the number of subcomponents that contribute appreciably and their weights, depend strongly on the values of a_i and q_i, in such a way that they will change in the stability region. All parameters are determined when the values β_i and G_{2n}^i are given. Several values of β_i and G_{2n}^i, corresponding to some typical values of a_i and q_i, are listed in [27]. In the table there, it is possible to see that in the first region for $a \ll q \ll 1$, we can assume that $G_2^i \cong G_{-2}^i$ and the rest of the coefficients $G_{\pm 2n}^i$, $n > 1$, can be ignored; thus, Eqs. (26) and (27) can be rewritten as

$$u_i^s(\tau) = u_{i0} \cos(\omega_i t + \delta_i), \qquad (28)$$

and

$$u_i^m(\tau) = C u_{i0} \cos \Omega t \cos(\omega_i t + \delta_i); \qquad (29)$$
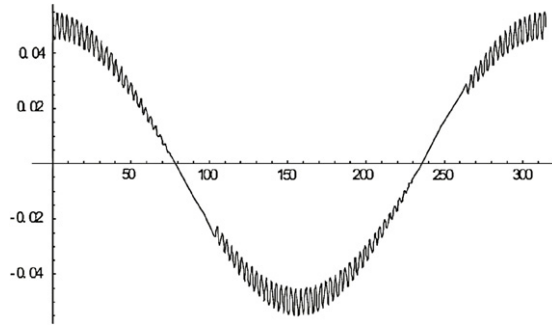
Fig. 4. Micro motion and secular motion of a trapped ion with parameters $q = 0.2$, $\beta = 0.02$. The oscillations at high frequency are the micro motion and those at low frequency are the secular motion.

or in other words,

$$u_i(t) = u_{i0} \cos(\omega_i t + \delta_i)(1 + C \cos \Omega t), \tag{30}$$

with

$$u_{i0}^2 = A_i'^2 + B_i'^2, \tag{31}$$

$$\delta = \arccos\left(\frac{A_i'}{\sqrt{A_i'^2 + B_i'^2}}\right), \tag{32}$$

and $C = 2G_2^i$.

In Fig. 4, we plot Eq. (30). The ion motion is composed of two types of oscillations: the harmonic oscillation with frequency ω_i, called secular motion, and the small contributions oscillating at a frequency Ω, called micromotion. Usually, the micromotion is ignored, but it can be reduced using additional electrodes [28]. In this way, the ion motion is controlled by Eq. (28) and behaves as it was confined in a harmonic pseudo-potential, that for the radial part, has the form

$$\Phi_r = \frac{m}{2}\left(\omega_x^2 x^2 + \omega_y^2 y^2\right). \tag{33}$$

Typically $U_0 = 0$, thus $a = 0$ (Eq. (14)); in any case, we are working in the region where $a \sim 0$. Thus, the frequencies ω_x and ω_y are degenerated, and Eq. (33) reduces to

$$\Phi_r = \frac{m\omega_r^2}{2}\left(x^2 + y^2\right). \tag{34}$$

To obtain an expression for ω_r, we can use the approximation [29],

$$\beta_r = \sqrt{a_r + \frac{q_r^2}{2}}, \tag{35}$$

with the definition $\omega_r = \beta_r \Omega/2$, to get

$$\omega_r = \frac{\Omega q_r}{2^{3/2}} = \frac{eV_0}{\sqrt{2}mr_0^2\Omega}. \tag{36}$$

Experimentally, the typical ranges of operation are $V_0 \approx 300$–800 V, $\Omega/2\pi \approx 16$–18 MHz, and $r_0 \approx 1.2$ mm, that gives a radial frequency $\omega_r \approx 1.4$–2.0 MHz for calcium ions (^{40}Ca$^+$).

We can summarize this section, saying that under certain conditions it is a good approximation to treat the ion motion as a harmonic oscillator. This allows us to apply algebraic techniques well known for this system to the ion–laser interaction in the following. In particular, invariant methods [30–32] permit the handling of time dependent systems in a simple way.

3. Ion–laser interaction in a trap with time-independent frequency

Despite the relative simplicity of the ion–laser interaction, the full theoretical treatment of its dynamics is a nontrivial problem, because this interaction is highly nonlinear. Even in the simplest case, where only a single ion is in the trap, one is usually forced to employ physically motivated approximations in order to find a solution. A well-known example is the *Lamb-Dicke* approximation, in which the ion is considered to be confined within a region much smaller than the laser wavelength. Many treatments also assume a *weak coupling* approximation; i.e., a sufficiently weak laser–ion coupling constant. Under

these conditions, tuning the laser frequency to integer multiples of the trap frequency results in effective Hamiltonians of the Jaynes–Cummings type [18–23], in which the center-of-mass of the trapped ion plays the role of the field mode in cavity QED. Recently, a new approach to this problem has been suggested, based on the application of a unitary transformation $\hat{T}$ that linearizes the total ion–laser Hamiltonian. Under this transformation the Hamiltonian becomes *exactly* equivalent to the classic Jaynes–Cummings model (JCM), including counter-rotating terms and an extra atomic driving term. Remarkably, the ion-trap system is thus formally equivalent to an atom interacting with a single-mode quantized electromagnetic field.

This equivalence does not of course lead to an exact solution to the ion-trap problem, since the complete JCM is also notoriously unsolved. To our knowledge, eigenstates and eigenvalues for this model have only ever been obtained either numerically or expressed in the form of a series with no known closed expression. Still, some advantages can be taken of regimes where the JCM is analytically, albeit approximately, soluble, such as the well-known "weak-coupling" limit where the rotating-wave approximation can be made. Using the already mentioned map $\hat{T}^{\dagger}$ to translate this solution back into the ion-trap scenario has led to the identification of a new soluble regime for that system. This in turn has already proven useful in the context of quantum computing. In this section, we study the interaction of a laser with a trapped ion in a harmonic potential with constant frequency. We start with the Hamiltonian of the system, and we show that it is possible to find Jaynes–Cummings type transitions and anti-Jaynes–Cummings type transitions, depending on the different cases of resonance and laser intensities that induce the coupling between the ion internal states and the ion vibrational states.

We can write the Hamiltonian of the trapped ion as

$$H = H_{\text{vib}} + H_{\text{at}} + H_{\text{int}}, \tag{37}$$

where H_{vib} is the ion's center of mass vibrational energy, H_{at} is the ion's internal energy, and H_{int} is the interaction energy between the ion and the laser. As we explained in the previous section, the vibrational motion can be fairly approximated by a harmonic oscillator. Internally, the ion will be modeled by a two level system. In the interaction between the ion and the laser, we will make the dipolar approximation, so we will write the interaction energy as $-e\vec{r} \cdot \vec{E}$, where $-e\vec{r}$ is the dipolar momentum of the ion and $\vec{E}$ is the electric field of the laser, that will be considered a plane wave. Thus, we write the Hamiltonian explicitly as

$$H = \nu\hat{n} + \frac{\omega_{21}}{2}\sigma_z + \lambda E_0 \left[e^{i(kx-\omega t)}\sigma_+ + e^{-i(kx-\omega t)}\sigma_- \right]. \tag{38}$$

The first term in the Hamiltonian is the ion vibrational energy; in the ion vibrational energy, the operator $\hat{n} = \hat{a}^{\dagger}\hat{a}$ is the number operator, and the ladder operators $\hat{a}$ and $\hat{a}^{\dagger}$ are given by the expressions

$$\hat{a} = \sqrt{\frac{\nu}{2}}\hat{x} + i\frac{\hat{p}}{\sqrt{2\nu}} \tag{39}$$

and

$$\hat{a}^{\dagger} = \sqrt{\frac{\nu}{2}}\hat{x} - i\frac{\hat{p}}{\sqrt{2\nu}}, \tag{40}$$

where we have made the ion mass equal to 1. Also, for simplicity, we have displaced the vibrational Hamiltonian by $\nu/2$, the vacuum energy, that in this case is not important.

The second term in the Hamiltonian corresponds to the ion internal energy; the matrices σ_z, σ_+, and σ_- are the Pauli matrices, and obey the commutation relations

$$[\sigma_z, \sigma_{\pm}] = \pm 2\sigma_{\pm}, \qquad [\sigma_+, \sigma_-] = \sigma_z, \tag{41}$$

and ω_{21} is the transition frequency between the ground state and the excited state of the ion.

Finally, the third term, is the interaction energy between the ion and the laser; in this last term, we have used again the rotating wave approximation.

3.1. Exact eigenstates

In this subsection we show that, under certain combinations of system parameters, it is possible to obtain *exact* eigenstates for the ion-trap Hamiltonian. Using the map $\hat{T}$ we also obtain therefore exact eigenstates of the complete JCM. The set of states we construct is by no means complete, and it is also unclear at present how (or if) it may be extended. Nevertheless, we believe that its existence may provide a clue to a deeper understanding of both models.

Let us start by recalling the equivalence between the ion-trap system and the JCM [18–23,33]. The Hamiltonian for the ion–laser interaction can be written as

$$H_{\text{ion}} = \nu\hat{n} + \frac{\delta}{2}\sigma_z + \Omega\left(\sigma_+\hat{D}(i\eta) + \sigma_-\hat{D}^{\dagger}(i\eta)\right), \tag{42}$$

where $\hat{D}(i\alpha) = e^{i\alpha(\hat{a}+\hat{a}^\dagger)}$ [34] is the displacement operator, ν the harmonic trapping frequency, $\delta = \omega_{21} - \omega$ the laser–ion detuning, Ω the (real) Rabi frequency of the ion–laser coupling and

$$\eta = K\sqrt{\frac{1}{2m\nu}} \tag{43}$$

is the so-called Lamb-Dicke parameter, that is a measure of the amplitude of the oscillations of the ion with respect to the wavelength of the laser field represented by its wave vector K.

On the other hand, the Jaynes–Cummings Hamiltonian with counter-rotating terms is given by

$$H_{JCM} = \omega\hat{n} + \frac{\omega_0}{2}\sigma_z + i\lambda(\sigma_+ + \sigma_-)(\hat{a} - \hat{a}^\dagger). \tag{44}$$

Although these two models appear to be physically and mathematically quite distinct, they are in fact exactly equivalent. The easiest way to see this is by rewriting Eq. (42) in a notation where operators acting on the internal ionic levels are represented explicitly in terms of their matrix elements, as

$$H_{\mathrm{ion}} = \begin{pmatrix} \nu\hat{n} + \dfrac{\delta}{2} & \Omega\hat{D}(i\eta) \\ \Omega\hat{D}^\dagger(i\eta) & \nu\hat{n} - \dfrac{\delta}{2} \end{pmatrix}. \tag{45}$$

Consider now the unitary operator

$$T = \frac{1}{\sqrt{2}} \begin{pmatrix} \hat{D}^\dagger(\beta) & \hat{D}(\beta) \\ -\hat{D}^\dagger(\beta) & \hat{D}(\beta) \end{pmatrix}, \tag{46}$$

where $\beta = i\eta/2$. It is possible to check after some algebra that

$$\mathcal{H}_{\mathrm{ion}} = TH_{\mathrm{ion}}T^\dagger = \begin{pmatrix} \nu\hat{n} + \Omega + \dfrac{\nu\eta^2}{4} & \dfrac{\iota\eta\nu}{2}(\hat{a} - \hat{a}^\dagger) + \dfrac{\delta}{2} \\ \dfrac{\iota\eta\nu}{2}(\hat{a} - \hat{a}^\dagger) + \dfrac{\delta}{2} & \nu\hat{n} - \Omega + \dfrac{\nu\eta^2}{4} \end{pmatrix}. \tag{47}$$

Returning to the usual notation, we obtain

$$\mathcal{H}_{\mathrm{ion}} = \nu\hat{n} + \Omega\sigma_z + \frac{\iota\eta\nu}{2}(\sigma_+ + \sigma_-)(\hat{a} - \hat{a}^\dagger) + \frac{\delta}{2}(\sigma_+ + \sigma_-) + \frac{\nu\eta^2}{4}. \tag{48}$$

Comparing with Eq. (44), it can be seen that this is precisely the Jaynes–Cummings interaction, supplemented by two additional terms: the first corresponds to an extra static electric field interacting with the atomic dipole, and the second is just a constant energy shift which can be disregarded. In particular, a purely Jaynes–Cummings form is recovered when $\delta = 0$, corresponding to a resonant laser–ion interaction in Eq. (42). Of course, in Eq. (48) various parameters in the Hamiltonian have different meanings than they do in Eq. (42): ν becomes the cavity field frequency ω, 2Ω the atomic transition frequency ω_0, δ the coupling strength with the static field and η the ratio between the Jaynes–Cummings Rabi frequency 2λ and the cavity frequency ω. In what follows, we shall refer to Eq. (48) as the 'Jaynes–Cummings picture' of the ion-trap Hamiltonian, Eq. (42).

This correspondence is very useful, since it enables one to map interesting properties of each model onto their counterparts in the other. For instance, it has been recently used to identify the existence of "super-revivals" in the ion–laser interaction [33], and to discover a means of realizing substantially faster logic gates for quantum information processing in a linear ion chain [35]. In this paper, we will use it to map eigenstates of one model into those of the other (it is clear that, if $|\psi\rangle$ is an eigenstate of H_{ion}, then $T|\psi\rangle$ is a corresponding one for $\mathcal{H}_{\mathrm{ion}}$). In this regard it is important to point out that, although H_{ion} and $\mathcal{H}_{\mathrm{ion}}$, both describe systems consisting of a two-level atom interacting with a bosonic mode, one should not identify each of these subsystems with their counterparts after the transformation has been applied. This is due to the fact that T is an *entangling* transformation: ion-trap states, where the ion's internal and vibrational degrees of freedom have well-defined pure states, can be mapped into entangled atom-cavity states in the corresponding cavity QED system.

3.1.1. Simple ansatz

Let us return now to the ion-trap Hamiltonian, Eq. (42). We will construct an *ansatz* which allows the determination of exact eigenstates of this system, provided certain relations are satisfied between the parameters Ω, δ, and η. In order to motivate our general solution, let us consider first the possibility of finding such a state of the form

$$|\psi\rangle = |e\rangle(c_0|0\rangle + c_1|1\rangle) + |g\rangle|\phi\rangle \equiv \begin{pmatrix} c_0|0\rangle + c_1|1\rangle \\ |\phi\rangle \end{pmatrix}, \tag{49}$$

where again we choose a notation where the ionic elements are written out explicitly (e.g., $\left(\begin{smallmatrix} |e\rangle=1 \\ 0 \end{smallmatrix} \right)$). Let us now see whether the eigenvalue equation

$$H_{\text{ion}} |\psi\rangle = E |\psi\rangle , \tag{50}$$

can be satisfied. Eq. (45) shows that this requires $|\phi\rangle$ to be of the form

$$|\phi\rangle = D^{\dagger} (i\eta) (d_0 |0\rangle + d_1 |1\rangle) = d_0 |-i\eta\rangle + d_1 |-i\eta; 1\rangle , \tag{51}$$

where $|-i\eta\rangle$ is a coherent state and $|\alpha; k\rangle \equiv \hat{D} (\alpha) |k\rangle$ is a displaced number state [36]. We thus require

$$H_{\text{ion}} |\psi\rangle = \begin{pmatrix} \left(c_0 \dfrac{\delta}{2} + \Omega d_0 \right) |0\rangle + \left(\Omega d_1 + c_1 \left(\nu + \dfrac{\delta}{2} \right) \right) |1\rangle \\ \left(c_0 \Omega + d_0 \left(\nu \hat{n} - \dfrac{\delta}{2} \right) \right) |-i\eta\rangle + \left(c_1 \Omega + d_1 \left(\nu \hat{n} - \dfrac{\delta}{2} \right) \right) |-i\eta; 1\rangle \end{pmatrix} . \tag{52}$$

Now, using the well-known fact that $\hat{D}^{\dagger} (\alpha) \hat{a} \hat{D} (\alpha) = \hat{a} + \alpha$ [34], it is easy to show that the displaced number states satisfy the recursion relation

$$\hat{n} |\alpha; k\rangle = (|\alpha|^2 + k) |\alpha; k\rangle + \alpha \sqrt{k + 1} |\alpha; k + 1\rangle + \alpha^* \sqrt{k} |\alpha; k - 1\rangle . \tag{53}$$

Substituting then Eqs. (49), (52) and (53) into Eq. (50) gives the following eigenstate conditions:

$$d_1 = 0; \qquad c_0 = \frac{\Omega}{\nu}; \qquad c_1 = \frac{i\eta\nu}{\Omega}; \qquad E = \nu + \frac{\delta}{2}, \tag{54}$$

which hold however *only if* the parameters Ω, δ, η satisfy the additional constraint

$$\left(\frac{\Omega}{\nu} \right)^2 + \eta^2 = 1 + \frac{\delta}{\nu}. \tag{55}$$

Under these conditions the state

$$\left| \psi_{\text{ion}}^+ \right\rangle = |e\rangle \left(\frac{\Omega}{\nu} |0\rangle + \frac{i\eta\nu}{\Omega} |1\rangle \right) + |g\rangle |-i\eta\rangle \tag{56}$$

is an (unnormalized) eigenstate of H_{ion} with eigenvalue $\nu + \delta/2$. Using operator $\hat{T}$ we can map this state into an eigenstate of the generalized JCM model in Eq. (48)

$$\left| \psi_{\text{JCM}}^+ \right\rangle = \hat{T} \left| \psi_{\text{ion}}^+ \right\rangle = |-\rangle \left(\frac{\Omega}{\nu} |-i\eta/2\rangle + \frac{i\eta\nu}{\Omega} |-i\eta/2; 1\rangle \right) + |+\rangle |-i\eta/2\rangle \tag{57}$$

where $|\pm\rangle = (|g\rangle \pm |e\rangle) / \sqrt{2}$.

Condition (55) means that the *ansatz* in Eq. (49) does not always succeed, as only two of the three parameters Ω, δ, η can be chosen independently. In addition, the domain of some of these parameters is not entirely unrestricted; for instance, it is easily seen that no solution exists when the laser is tuned such that $\delta < -2\nu$. Nevertheless, the existence of solutions satisfying Eq. (49) leads us naturally to seek for other solutions using similar or slightly generalized ansatz. For example, a second solution can be easily found if we note that the Hamiltonian H_{ion} is invariant under the combined transformations

$$|e\rangle \leftrightarrow |g\rangle, \qquad \delta \leftrightarrow -\delta, \qquad \eta \leftrightarrow -\eta. \tag{58}$$

Applying this symmetry transformation also to Eqs. (54) and (55) we can see that, as long as we satisfy the condition

$$\left(\frac{\Omega}{\nu} \right)^2 + \eta^2 = 1 - \frac{\delta}{\nu}, \tag{59}$$

then

$$\left| \psi_{\text{ion}}^- \right\rangle = |e\rangle |i\eta\rangle + |g\rangle \left(\frac{\Omega}{\nu} |0\rangle - \frac{i\eta\nu}{\Omega} |1\rangle \right) \tag{60}$$

is an eigenstate with eigenvalue $\nu - \delta/2$.

Note that, unless $\delta = 0$, conditions (55) and (59) are *mutually exclusive*. (In the 'ion-trap' picture, this means that the laser must be resonant with the ion and in the 'JCM' picture, that no static field is applied; i.e., that the Hamiltonian is just the full JCM). In other words, only in this special case are $\left| \psi_{\text{ion}}^+ \right\rangle$ and $\left| \psi_{\text{ion}}^- \right\rangle$ simultaneous (in fact, degenerate) eigenstates of H_{ion}. The reason is that, in this case only, the ion-trap Hamiltonian, Eq. (42), has an extra symmetry: it commutes with the operator $\sigma_x \exp(i\pi \hat{a}^{\dagger} \hat{a})$. This parity-like observable has two eigenvalues ± 1, and so the spectrum of H_{ion} is two-fold degenerate (in the JCM picture, the corresponding symmetry operator is $\sigma_z \exp(i\pi \hat{a}^{\dagger} \hat{a})$). It can be easily checked that neither $\left| \psi_{\text{ion}}^+ \right\rangle$ nor $\left| \psi_{\text{ion}}^- \right\rangle$ have this symmetry, but simple linear combinations of them do.

3.1.2. General ansatz

One can easily generalize Eq. (56) to obtain a more general eigenstate for H_{ion}; this general state can be proposed as

$$|\psi\rangle = \frac{\Omega}{\nu} \sum_{n=0}^{m+1} c_n |n\rangle |e\rangle + \sum_{n=0}^{m} d_n |-i\eta, n\rangle |g\rangle . \tag{61}$$

Substituting this proposal in the eigenvalue equation (50), it can be shown that the corresponding eigenvalues are $E_m = (m+1)\nu + \frac{\delta}{2}$, that

$$c_n = \begin{cases} \dfrac{1}{m+1-n} \dfrac{\nu^2}{\Omega^2} d_n; & n = 0, 1, 2, \ldots, m \\ i\eta \dfrac{\nu^2}{\Omega^2} \sqrt{m+1} d_m; & n = m+1 \end{cases} \tag{62}$$

and that the d_n coefficients satisfy

$$\begin{bmatrix} \varepsilon_0 & -i\eta & & & \\ i\eta & \varepsilon_1 & -i\sqrt{2}\eta & & \\ 0 & i\sqrt{2}\eta & \ddots & \ddots & \\ & & \ddots & \varepsilon_{m-1} & -i\sqrt{m}\eta \\ & & & i\sqrt{m}\eta & \varepsilon_m \end{bmatrix} \begin{bmatrix} d_0 \\ \vdots \\ d_m \end{bmatrix} = \vec{0} \tag{63}$$

where

$$\varepsilon_n = 1 + m - n - \eta^2 + \frac{\delta}{\nu} - \frac{1}{1+m-n} \frac{\Omega^2}{\nu^2}. \tag{64}$$

Eq. (63) establish the recurrence relations

$$i\sqrt{j}\eta d_{j-1} + \varepsilon_j d_j - i\sqrt{j+1}\eta d_{j+1} = 0, \quad j = 0, 1, 2, \ldots, m-1 \tag{65}$$
$$i\sqrt{m}\eta d_{m-1} + \varepsilon_m d_m = 0$$

that allow us to calculate all the d coefficients of the eigenvector (61) in terms of d_0. The first ones are given by

$$d_1 = -i\varepsilon_0 \frac{d_0}{\eta} \tag{66}$$

$$d_2 = \left(\eta^2 - \varepsilon_0\varepsilon_1\right) \frac{d_0}{\sqrt{2}\eta^2}$$

$$d_3 = -i\left(2\eta^2\varepsilon_0 + \eta^2\varepsilon_2 - \varepsilon_0\varepsilon_1\varepsilon_2\right) \frac{d_0}{\sqrt{6}\eta^3}$$

$$d_4 = \left(3\eta^4 - 3\eta^2\varepsilon_0\varepsilon_1 - 2\eta^2\varepsilon_0\varepsilon_3 - \eta^2\varepsilon_2\varepsilon_3 + \varepsilon_0\varepsilon_1\varepsilon_2\varepsilon_3\right) \frac{d_0}{2\sqrt{6}\eta^4}.$$

Note that the vector of coefficients $(d_0, \ldots, d_m)$ is an eigenvector of this tridiagonal matrix with zero eigenvalue. This is only possible if the determinant of the matrix in Eq. (63) is zero, which imposes a constraint on Ω, δ, ν. These imposed conditions are the generalization of Eq. (55).

It is easy to show that if $\Omega \ll \nu, \eta \ll 1$ and $\delta = -\nu$ all these conditions are satisfied (the matrix in Eq. (63) becomes diagonal with a zero in the $m+1, m+1$ position), and then we obtain the *exact* eigenvalues and the *exact* eigenvectors without using the rotating wave approximation.

As we already mention, the Hamiltonian is symmetric under the combined transformations $\{|e\rangle \leftrightarrow |g\rangle ; \delta \leftrightarrow -\delta; \eta \leftrightarrow -\eta\}$; this allows us to propose another set of eigenstates as

$$|\psi\rangle = \sum_{n=0}^{m} d_n |i\eta, n\rangle |e\rangle + \frac{\Omega}{\nu} \sum_{n=0}^{m+1} c_n |n\rangle |g\rangle , \tag{67}$$

where now

$$c_n = \begin{cases} \dfrac{1}{m+1-n} \dfrac{\nu^2}{\Omega^2} d_n; & n = 0, 1, 2, \ldots, m \\ -i\eta \dfrac{\nu^2}{\Omega^2} \sqrt{m+1} d_m; & n = m+1. \end{cases} \tag{68}$$

The d coefficients satisfy Eq. (63) but with

$$\varepsilon_n = \frac{\delta}{\nu} + \frac{1}{1 + m - n} \frac{\Omega^2}{\nu^2} - 1 - m + n + \eta^2, \tag{69}$$

and the corresponding eigenvalues are $E_m = (m+1)\nu - \frac{\delta}{2}$.

In this case all the constraints imposed by Eq. (63) are satisfied if $\Omega \ll \nu$, $\eta \ll 1$ and $\delta = \nu$, and the *exact* eigenvalues and the *exact* eigenvectors are again obtained without using the rotating wave approximation.

3.2. Blue and red sidebands

Processes where simultaneously the internal excitation and the motional quantum numbers are increased (decreased) are known as blue sideband excitations [37]. When simultaneously the internal excitation is excited (lowered) and the motional quantum numbers are decreased (increased) are known as the red sideband. We discuss now some properties of the eigenstates (61) and (67) in order to show that, under certain conditions, namely, low intensity ($\Omega \ll \nu$) and Lamb-Dicke ($\eta \ll 1$) regimes, eigenstates (61) correspond to the blue side band and the eigenstates (67) correspond to the red side band. Under these conditions, it is easy to prove that

$$|\psi_0\rangle \approx i\eta \frac{\nu}{\Omega} |1\rangle |e\rangle + |0\rangle |g\rangle, \tag{70}$$

which is an eigenstate of the operator of the form $\sigma_+ \hat{a}^\dagger + \sigma_- \hat{a}$. Thus, when an up ion internal transition takes place ($|g\rangle \longrightarrow |e\rangle$) the vibrational motion acquires an extra phonon ($|0\rangle \longrightarrow |1\rangle$). In general, we will have in this approximation

$$|\psi_m\rangle \approx i\sqrt{1 + m} \eta \frac{\nu}{\Omega} d_m |m+1\rangle |e\rangle + \sum_{n=0}^{m} d_n |n\rangle |g\rangle \tag{71}$$

showing that internal up transitions are accompanied by vibrational up transitions.

In the case of the eigenstates (67), we have the conditions $\Omega \ll \nu$, $\eta \ll 1$ and $\delta = \nu$. Under these conditions we can approximate the eigenstates as

$$|\psi_m\rangle \approx \sum_{n=0}^{m} d_n |n\rangle |e\rangle - i\sqrt{1 + m} \eta \frac{\nu}{\Omega} d_m |m\rangle |g\rangle. \tag{72}$$

Thus transitions to the lower internal ion states are associated with an increase of vibrational quanta.

3.3. The blue side band and the red side band by means of the intensity

In the resonant case, processes that correspond to the blue side band and the red side band can also be obtained by means of the laser intensity. If we take $\delta = 0$, and consider the Lamb-Dicke limit, the displacement operator can be expanded in Taylor series and written as

$$\hat{D}(\alpha) = e^{\alpha \hat{a}^\dagger - \alpha^* \hat{a}} \approx 1 + \alpha \hat{a}^\dagger - \alpha^* \hat{a}, \tag{73}$$

such that the Hamiltonian (45) reads

$$H = \nu \hat{n} + \Omega \sigma_x - \Omega \eta \sigma_y \left(\hat{a} + \hat{a}^\dagger \right), \tag{74}$$

where we have used that $\sigma_x = \sigma_+ + \sigma_-$ and $\sigma_y = -i(\sigma_+ - \sigma_-)$. By making now a rotation around the Y axis (by means of the transformation $\exp(i\frac{\pi}{4}\sigma_y)$), and going to the interaction picture, we get the transformed Hamiltonian

$$H_I = i\eta\Omega \left[e^{-it(\nu - 2\Omega)} \hat{a}\sigma_+ - e^{it(\nu - 2\Omega)} \sigma_- \hat{a}^\dagger - e^{-it(\nu + 2\Omega)} \hat{a}\sigma_- + e^{it(\nu + 2\Omega)} \sigma_+ \hat{a}^\dagger \right]. \tag{75}$$

If we take now $\nu = -2\Omega$, and we use the rotating wave approximation, the Hamiltonian reduces to

$$H_I = -i\eta\Omega \left(\hat{a}\sigma_- - \sigma_+ \hat{a}^\dagger \right) \tag{76}$$

which clearly gives us the blue side band.

To get the red side band, we must take $\nu = 2\Omega$ and the Hamiltonian we get is

$$H_I = i\eta\Omega \left(\hat{a}\sigma_+ - \sigma_- \hat{a}^\dagger \right) \tag{77}$$

that clearly implies that when the ion goes from the ground internal state to the internal excited state, the vibrational motion loses one phonon and vice versa; i.e., the red sideband.

4. Solution in different regimes: dispersive Hamiltonians

The ion–laser interaction may be easily solved in the low intensity regime [38–42], but besides the condition that the laser intensity is much lower than the vibrational frequency, we set the condition that the detuning between the laser and the atomic transition frequency is an integral multiple of the vibrational frequency. Then some questions arise: Is it possible not to consider integer multiples of the vibrational frequency? Is it possible to solve for high and middle intensities?

We have shown in Section 3 that it is possible to find solutions for any set of parameters; i.e., in all regimes [43]. However, the solutions are not general because the set of eigenstates that may be found cannot expand all possible (general) states.

It has been shown already that for low intensities it is possible also to consider the ion micromotion [26], and by using Ermakov–Lewis invariant methods [30–32] it was possible to *linearize* the ion–laser Hamiltonian when the micromotion was included [44]. Here, we follow Zúñiga-Segundo et al. [45] and show how it is possible to solve the ion–laser interaction in different regimes, including high intensity and medium intensity.

4.1. Different regimes

In Section 3.1, we showed that the ion–laser Hamiltonian (45) can be casted in the form given by expression (48) by means of the similarity transformation (46). Therefore, we have *linearized* the ion–laser interaction in an exact way, by means of a unitary transformation; i.e., both Hamiltonians, $\hat{H}_{\text{ion}}$ and $\hat{\mathcal{H}}_{\text{ion}}$ are equivalent. In the following, we will neglect the term $\frac{\nu\eta^2}{4}$ because it only represents a constant shift of all the eigenenergies. Of course, transformation (46) has to be applied to an initial condition for the internal state of the ion and its vibrational motion wave function. Let us assume that we have the initial state

$$|\psi(0)\rangle = |i\alpha\rangle|e\rangle, \tag{78}$$

where $|i\alpha\rangle$ is a coherent state, and for simplicity we take α a real number (to avoid extra phases later, but the calculation may be done for complex α). Then, we have that the initial wave function associated with the transformed Hamiltonian (48) is

$$|\tilde{\psi}(0)\rangle = T|\psi(0)\rangle, \tag{79}$$

where the transformation T is given in (46). If we write the initial wave function in terms of 2×2 matrices, we obtain

$$|\tilde{\psi}(0)\rangle = \frac{1}{\sqrt{2}}e^{i\hat{n}\frac{\pi}{2}}\begin{pmatrix} \hat{D}^{\dagger}(i\eta/2) & \hat{D}(i\eta/2) \\ -\hat{D}^{\dagger}(i\eta/2) & \hat{D}(i\eta/2) \end{pmatrix}\begin{pmatrix} |i\alpha\rangle \\ 0 \end{pmatrix} = \frac{e^{i\hat{n}\frac{\pi}{2}}}{\sqrt{2}}\begin{pmatrix} |i(\alpha-\eta/2)\rangle \\ -|i(\alpha-\eta/2)\rangle \end{pmatrix}. \tag{80}$$

Thus, we have changed the complicated Hamiltonian (45) by the linear Hamiltonian (48) via a unitary transformation. The small price we have to pay, is that in the initial wave function the coherent state is displaced and the ion is initially (in the new frame) in a superposition of ground and excited states.

### 4.2. Medium intensity regime (MIR)

We already considered this case, when we analyzed in Section 3.3 the blue and red side bands by means of the intensity. In this case, the vibrational frequency is of the order of twice the field intensity (Rabi frequency). We also consider the Lamb-Dicke regime; i.e., $\eta \ll 1$. For simplicity, we will set $\delta = 0$ to show the different possibilities we have now. However, it is not difficult to produce effective Hamiltonians also in the off-resonance case. In this case, the Hamiltonian (48) may be casted into (77) which is a Hamiltonian that has been extensively studied [18,22]; therefore, we will not add more here, except the fact that for the medium intensity regime the Hamiltonian (45) may be exactly expressed as a JCM Hamiltonian via a unitary transformation and the rotating wave approximation, without extra approximations.

4.3. Low and high intensity regimes

In the case of the low intensity regime (LIR) the solution has been known already for several years [16,17]; however, we will treat it with some details in Section 5. Here, we will show a different method that is also valid for the high intensity regime (HIR). Just for the matter of qualitative analysis, let us take $\delta = 0$. Consider now $\Omega \ll \nu$ (LIR) or $\Omega \gg \nu$ (HIR) in Eq. (48). As this Hamiltonian for $\delta = 0$ is equivalent to the atom-field interaction, we can borrow knowledge from such an interaction: we know that when the field and atomic transition frequencies are very different (in our case, it is translated in the equation $|\nu - 2\Omega| \ll \eta\nu/2$, that may happen in either of both regimes, HIR or LIR), atom and field stop to exchange energy and we obtain a dispersive Hamiltonian [46]. The same happens in the ion–laser interaction, and via a small rotation approach [47], we will be able to cast Hamiltonian (48) as an effective (dispersive) Hamiltonian.

By transforming the Hamiltonian (48) with the unitary operators

$$\hat{U}_1 = e^{\xi_1(\hat{a}^{\dagger}\hat{\sigma}_+ - \hat{a}\hat{\sigma}_-)}, \qquad \hat{U}_2 = e^{\xi_2(\hat{a}\hat{\sigma}_+ - \hat{a}^{\dagger}\hat{\sigma}_-)}; \tag{81}$$
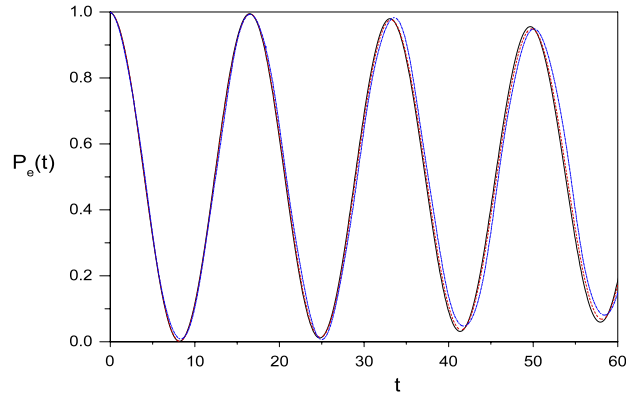
Fig. 5. Plot of $P_e(t)$ as a function of t for $k = 0$, $\nu = 1$, $\Omega = 0.2$ and $\eta = 0.1$. The vibrational motion of the ion is considered to be in a coherent state, $|\alpha|^2 = 4$ and the ion in its excited state. Solid line represents the numerical (exact) solution, dashed line the solution from Section 3 and the dot-dashed line the solution for the dispersive Hamiltonian.

i.e.,

$$\hat{\mathcal{H}}_{\text{eff}} = \hat{U}_2 \hat{U}_1 \hat{\mathcal{H}}_{\text{ion}} \hat{U}_1^\dagger \hat{U}_2^\dagger \tag{82}$$

with $\xi_1, \xi_2 \ll 1$, using

$$\xi_1 = \frac{\eta \nu}{2(\nu + 2\Omega)} \qquad \xi_2 = \frac{\eta \nu}{2(2\Omega - \nu)}, \tag{83}$$

and remaining up to first order in the expansion $e^{\xi A} B e^{-\xi A} = B + \xi[A, B] + \frac{\xi^2}{2!}[A, [A, B]] + \cdots \approx B + \xi[A, B]$ [47], we get the effective Hamiltonian

$$\hat{\mathcal{H}}_{\text{eff}} = \nu \hat{a}^\dagger \hat{a} + \Omega \hat{\sigma}_z - \chi_{\text{ion}} \hat{\sigma}_z \left(\hat{a}^\dagger \hat{a} + \frac{1}{2} \right) + \frac{\delta}{2}(\sigma_+ + \sigma_-) + \frac{\kappa}{2} \hat{\sigma}_z \left(\hat{a}^\dagger + \hat{a} \right), \tag{84}$$

that for $\delta = 0$ is known as the dispersive Hamiltonian. Note that, just as in the atom–field case, there is no need to transform the (already transformed) initial state (80) as a small rotation has been applied. We can see that in fact $\xi_1, \xi_2 \ll 1$ either in the LIR (in this case we have also to consider $\eta \ll 1$) or in the HIR (no constrain for η), which justifies completely the approximation for the above Hamiltonian. For the resonant case, $\delta = 0$, it becomes diagonal and we can solve it in an easy way.

In Fig. 5, we show a plot for the probability to find the ion in its excited state

$$P_e(t) = \langle \psi(0)|\hat{T}^\dagger \exp(it\hat{\mathcal{H}}_{\text{eff}})\hat{T}|e\rangle \langle e|\hat{T}^\dagger \exp(-it\hat{\mathcal{H}}_{\text{eff}})\hat{T}|\psi(0)\rangle \tag{85}$$

as a function of time for $k = 0$, $\nu = 1$, $\Omega = 0.2$ and $\eta = 0.1$. The vibrational motion of the ion is considered to be a coherent state $|\alpha|^2 = 4$, and the internal state of the ion is excited. The three curves in the figure correspond to the exact numerical solution (solid line), the solution from Hamiltonian (45) (dashed line) and the solution for the dispersive Hamiltonian (84). We can see excellent agreement among the three plots for the LIR. Now, for the HIR in Fig. 6, we show a plot also of $P_e(t)$ as a function of time for the exact numerical solution (solid line) and our solution from this section (dashed line), but now with the parameters for $k = 0$, $\Omega = 1$, $\nu = 0.2$, and $\eta = 0.1$. Again, it may be noticed the excellent agreement between both curves. We should stress that there is no other analytical solution to compare with, as ours is the first analytical solution in this regime (also in the medium intensity regime).

The new interaction constants in the effective Hamiltonian (84) have the forms
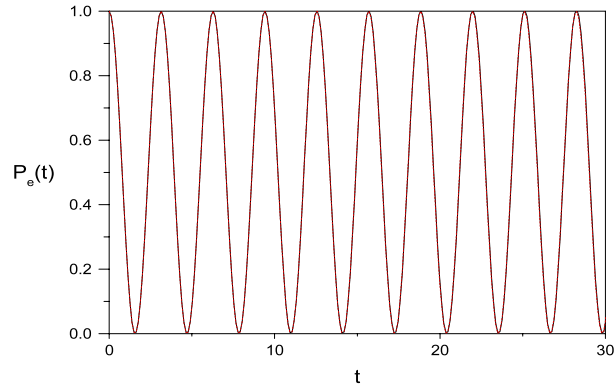
$$\chi_{\text{ion}} = \frac{2\eta^2 \nu^2 \Omega}{4\Omega^2 - \nu^2}, \qquad \kappa = \frac{\delta \eta \nu^2}{4\Omega^2 - \nu^2}. \tag{86}$$

In the resonant case and high intensity regime, $\Omega \gg \nu$, it is easy to show that

$$\chi_{\text{ion}} \to \chi^{\text{high}} = \frac{2\eta^2 \nu^2}{4\Omega} \frac{1}{1 - \frac{\nu^2}{4\Omega^2}} \approx \frac{\eta^2 \nu^2}{2\Omega}, \tag{87}$$

while in the low intensity regime, $\Omega \ll \nu$, we will have the same Hamiltonian, but χ will change to

$$\chi_{\text{ion}} \to \chi_{\text{low}} = -2\eta^2 \Omega \frac{1}{1 - \frac{4\Omega^2}{\nu^2}} \approx -2\eta^2 \Omega. \tag{88}$$

Fig. 6. Plot of $P_e(t)$ as a function of t for $k = 0$, $\Omega = 1$, $\nu = 0.2$ and $\eta = 0.1$. The vibrational motion of the ion is considered to be in a coherent state, $|\alpha|^2 = 4$ and the ion in its excited state. Solid line represents the numerical (exact) solution, dashed line the solution for the dispersive Hamiltonian.

If in Eq. (84) we take the detuning δ different from zero, we could get the usual blue and red side-bands interactions (see for instance Ref. [42]). This is done by choosing the value $\delta = \pm\nu$. The only case in which we can obtain such regimes is the low intensity case, where one can perform the rotating wave approximation to the Hamiltonian (84), which agrees with the usual procedure for obtaining such blue and red side-band regimes. The high intensity case, $\Omega \gg \nu$, does not allow such side-bands because in the Hamiltonian (84) the interaction constants multiplying the different terms may be of the same order.

5. Low intensity regime

If we consider that the Hamiltonian (38) corresponds to the wave function $|\xi(t)\rangle$, the Schrödinger equation can be written as

$$i\frac{\partial}{\partial t}|\xi\rangle = H|\xi\rangle. \tag{89}$$

Let us examine the transformation to a rotating frame of frequency ω, by means of the unitary transformation

$$T(t) = \exp\left(i\frac{\omega}{2}\sigma_z t\right). \tag{90}$$

Applying the transformation T, the wave function $|\xi(t)\rangle$ transforms into the wave function $|\phi(t)\rangle$; i.e.,

$$T(t)|\xi(t)\rangle = |\phi(t)\rangle, \tag{91}$$

and the Hamiltonian transforms into

$$H_T = i\frac{\partial T(t)}{\partial t}T^\dagger(t) + T(t)HT^\dagger(t). \tag{92}$$

Writing the position operator $\hat{x}$ in terms of the ladder operators, expressions (39) and (40), using the Baker–Hausdorff formula [26,48], and the commutators of the Pauli matrices (41), the explicit transformed Hamiltonian is

$$H_T = \nu\hat{n} + \nu\frac{k}{2}\sigma_z + \lambda E_0\left[e^{i\eta(\hat{a}^\dagger+\hat{a})}\sigma_+ + \text{H.C.}\right] \tag{93}$$

where η is the Lamb-Dicke parameter. The quantity

$$k\nu = \omega_{21} - \omega \tag{94}$$

is the detuning between the plane wave frequency and the transition frequency of the ion; in other words, we are considering that the detuning is a multiple integer of the vibrational frequency of the ion.

We need now to factorize the exponential in the Hamiltonian (93). As $[\hat{a}, [\hat{a}, \hat{a}^\dagger]] = 0$, and $[\hat{a}^\dagger, [\hat{a}, \hat{a}^\dagger]] = 0$, we can use the Baker–Hausdorff formula, and write

$$e^{-i\eta(\hat{a}+\hat{a}^\dagger)} = e^{-\eta^2/2}e^{-i\eta\hat{a}^\dagger}e^{-i\eta\hat{a}}. \tag{95}$$

Expanding in Taylor series the exponentials that contains the operators, and substituting in the Hamiltonian (93), we obtain

$$H_T = \nu\hat{n} + \nu\frac{k}{2}\sigma_z + \lambda E_0 e^{-\eta^2/2}\left[\sigma_-\sum_{n,m=0}^{\infty}\frac{(-i\eta)^{n+m}}{n!m!}(\hat{a}^\dagger)^n\hat{a}^m + \text{H.C.}\right]. \tag{96}$$

We go now to the interaction picture, using the transformation

$$T_{\text{free}} = \exp\left[it\left(v\hat{n} + \frac{kv}{2}\sigma_z\right)\right].$$ (97)

We apply this transformation, using the following two commutators,

$$[\hat{a}, f(\hat{a}, \hat{a}^\dagger)] = \frac{\partial f}{\partial \hat{a}^\dagger}$$ (98)

and

$$[\hat{a}^\dagger, f(\hat{a}, \hat{a}^\dagger)] = -\frac{\partial f}{\partial \hat{a}},$$ (99)

and we obtain

$$H_{\text{int}} = \Omega e^{-\eta^2/2}\left[\sigma_- \sum_{n,m=0}^{\infty} \frac{(-i\eta)^{n+m}}{n!m!}(\hat{a}^\dagger)^n \hat{a}^m e^{-i(n-m-k)vt} + \text{H.C.}\right],$$ (100)

where $\Omega = \lambda E_0$ is the exchange energy frequency of the internal and vibrational states, called Rabi frequency.

The interaction Hamiltonian (100) has a diversity of contributions, each contribution oscillates with a frequency that is a multiple integer of v. We apply now the rotating wave approximation; as the Schrödinger equation is a first order differential equation in time, we have to integrate it once with respect to time; this integration brings the sum and the difference of the frequencies to the denominator. The terms changing slowly will dominate over the terms changing very fast; so the contribution to the Hamiltonian of those fast terms is neglected, and only the slowly changing terms are kept. In this case, the terms that do not rotate quickly are those whose exponent satisfies the relation $n - m = k$, and as we already explained, are those terms that we will keep. This approximation is valid for

$$\Omega \ll v.$$ (101)

As Ω is proportional to the amplitude of the laser electric field, from (101) it is clear that this approximation is valid for low intensity. We have then,

$$H_{\text{int}} = \Omega e^{-\eta^2/2}\left[\sigma_- \sum_{m=0}^{\infty} \frac{(-i\eta)^{2m+k}}{(m+k)!m!}(\hat{a}^\dagger)^k (\hat{a}^\dagger)^m \hat{a}^m + \text{H.C.}\right].$$ (102)

Using now the fact that the number states is a complete set,

$$I = \sum_{n=0}^{\infty} |n\rangle\langle n|,$$ (103)

where I is the identity operator, we can write

$$(\hat{a}^\dagger)^m \hat{a}^m = (\hat{a}^\dagger)^m \hat{a}^m \sum_{j=0}^{\infty} |j\rangle\langle j| = \frac{\hat{n}!}{(\hat{n}-m)!} \sum_{j=0}^{\infty} |j\rangle\langle j| = \frac{\hat{n}!}{(\hat{n}-m)!},$$ (104)

that substituted in the Hamiltonian (102), gives us

$$H_{\text{int}} = \Omega e^{-\eta^2/2}\left[\sigma_-(\hat{a}^\dagger)^k (-i\eta)^k \sum_{m=0}^{\infty} \frac{(-i\eta)^{2m}}{(m+k)!m!} \frac{\hat{n}!}{(\hat{n}-m)!} + \text{H.C.}\right].$$ (105)

Using the explicit expression for the associated Laguerre polynomials [50,51],

$$L_n^{(\alpha)}(x) = \sum_{i=0}^{n} (-1)^i \frac{(n+\alpha)!}{(n-i)!(\alpha+i)!} \frac{x^i}{i!},$$

we can write

$$H_{\text{int}} = \Omega e^{-\eta^2/2}\left[\sigma_-(\hat{a}^\dagger)^k (-i\eta)^k \frac{\hat{n}!}{(\hat{n}+k)!} L_{\hat{n}}^{(k)}(\eta^2) + \text{H.C.}\right].$$ (106)

We will consider now processes where only one phonon is exchanged; that means that we must take $k = 1$ in the Hamiltonian (106). We will consider also that the oscillation amplitude of the ion is much smaller than the laser frequency; that is, $\eta \ll 1$, or in other words, we suppose the Lamb-Dicke regime. With these two considerations, the Hamiltonian (106) reduces to (the subscript jc stands for Jaynes–Cummings)

$$H_{\text{jc}} = -i\eta\Omega(\hat{a}^\dagger\sigma_- - \hat{a}\sigma_+).$$ (107)
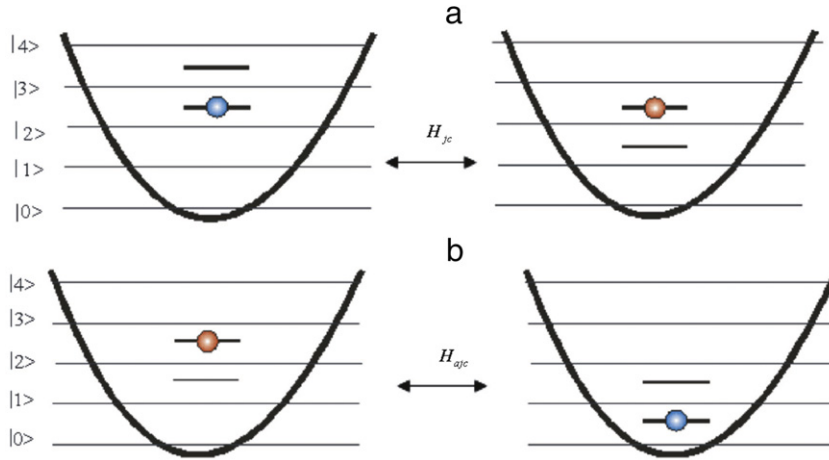
Fig. 7. (a) A Jaynes–Cummings Hamiltonian implies the ascent (descent) of one ion vibrational quantum, and at the same time, the transition from an excited (ground) internal state to the ground (excited) state. (b) An anti-Jaynes–Cummings Hamiltonian annihilate (creates) one quantum from the vibrational motion and transfers the ion internally from the excited (ground) state to the ground (excited) state.

In agreement with the considerations made above, the Hamiltonian (107) describes emission and absorption of one vibrational excitation, when the atom makes electronic transitions. The first term represents the absorption of a vibrational excitation and the transition of the ion from the excited state to the ground state. The second term represents the inverse process; the ion goes from the ground state to the excited state, annihilating one phonon, and the vibrational state decays in one quanta.

All this can be clearly seen, if we apply the Hamiltonian (107) to the correct states. In the first case, we have to apply the Hamiltonian to the state $|n\rangle|e\rangle$, which represents n vibrational quanta and the ion in the excited state $|e\rangle$; we get,

$$H_{jc}|n\rangle|e\rangle \propto |n+1\rangle|g\rangle; \tag{108}$$

which is the state with $n+1$ vibrational quanta, and the ion in the ground state. In the second case, the state is given by $|n+1\rangle|g\rangle$, and when we apply the Hamiltonian we obtain

$$H_{jc}|n+1\rangle|g\rangle \propto |n\rangle|e\rangle; \tag{109}$$

that is the state with n vibrational quanta, and the ion in the excited state.

We can repeat all the above procedures now when the laser frequency is greater than that of the transition

$$kv = \omega - \omega_{21}, \tag{110}$$

and obtain the Hamiltonian (clearly now, the subscript ajc stands for anti-Jaynes–Cummings)

$$H_{ajc} = -i\eta\Omega(\hat{a}\sigma_- - \hat{a}^\dagger\sigma_+). \tag{111}$$

In the first term, we have the annihilation of one quanta from the vibrational motion and the ion internal transition from the excited state to the ground state. In the second term, we have the creation of one vibrational quanta and the internal excitation of the ion from the ground state to the excited state. In Fig. 7, we explain why this Hamiltonian is anti-Jaynes–Cummings type.

Applying the anti-Jaynes–Cummings Hamiltonian to the adequate states, the previous comments can be easily understood. If we apply the Hamiltonian (111) to the state $|n\rangle|e\rangle$, we get

$$H_{ajc}|n\rangle|e\rangle = |n-1\rangle|g\rangle, \tag{112}$$

and if we apply it to the state $|n-1\rangle|g\rangle$, we get

$$H_{ajc}|n-1\rangle|g\rangle = |n\rangle|e\rangle. \tag{113}$$

From the point of view of the trapped ion, all this means that we can take it to its lowest energy vibrational state, alternating successively, and as many times as necessary, the detuning between the frequency of the plane wave and the internal frequency of the ion. Again, we can illustrate all this by applying the correct Hamiltonian to the adequate state. For that let us consider a vibrational state $|n\rangle$ and the ground internal state; if we apply the Hamiltonian (107), we get

$$H_{jc}|n\rangle|g\rangle = |n-1\rangle|e\rangle. \tag{114}$$

We apply now the Hamiltonian (111), obtaining

$$H_{ajc}|n-1\rangle|e\rangle = |n-2\rangle|g\rangle, \tag{115}$$

and the ion has lost two quanta of vibrational energy. Repeating successively this procedure, we can arrive to the state $|0\rangle|g\rangle$.
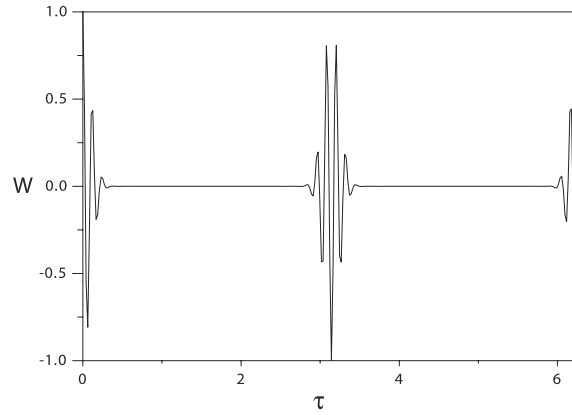
Fig. 8. Plot of the atomic inversion, $W(t) = P_2 - P_1$, the probability to find the ion in its excited state minus the probability to find it in the ground state, for an ion initially in its excited state and the vibrational state in a coherent state, with $\alpha = 5$.

5.1. Adding vibrational quanta

We now show how to generate nonclassical vibrational states in the low intensity regime. From Eq. (102) with $k = 2$, we note that if the Lamb-Dicke parameter is much less than one, $\eta \ll 1$, we can remain to the lowest order in the sum, such that we obtain the so-called two-phonon Hamiltonian

$$H_I = \epsilon[\sigma_- \hat{a}^2 + \sigma_+ \hat{a}^{\dagger 2}], \tag{116}$$

with $\epsilon = -\Omega/2$. For the study of the dynamics of interest, we need the time evolution described by the Hamiltonian (116). The advantage of the interactions of Jaynes–Cummings type consists in the fact that the Hamiltonian can easily be diagonalized, and using the same procedure that was already used, it is possible to show that

$$\hat{U}_I(t) = \sum_{m=0,1} |m\rangle|g\rangle\langle m|\langle g| + \sum_{n=0}^{\infty} \left[\cos\left(\frac{1}{2}\Omega_n t\right) (|n+2\rangle|g\rangle\langle n+2|\langle g| + |n\rangle|e\rangle\langle n|\langle e|) \right.$$
$$\left. - i \sin\left(\frac{1}{2}\Omega_n t\right) (|n+2\rangle|g\rangle\langle n|\langle e| + |n\rangle|e\rangle\langle n+2|\langle g|) \right]. \tag{117}$$

The quantity Ω_n is the two-phonon Rabi frequency which is given by

$$\Omega_n = 2\epsilon\sqrt{(n+1)(n+2)}. \tag{118}$$

Using these results, the time evolution of the quantum state in the interaction picture is easily derived for arbitrarily chosen initial conditions. We have

$$|\Psi(t)\rangle = \hat{U}_I(t)|\Psi(0)\rangle. \tag{119}$$

If we consider as initial state the ion in its excited state $|e\rangle$ and the vibrational state a coherent state, we can find the atomic inversion, (that we recall that it is defined as the probability to find the ion in its excited state minus the probability to find it in the ground state). Using (117) and (119), we get

$$W(t) = \exp\left(-|\alpha|^2\right) \sum_{n=0}^{\infty} \frac{|\alpha|^{2n}}{n!} \cos(2\Omega_n t). \tag{120}$$

We plot this function in Fig. 8 as a function of the scaled time $\tau = \epsilon t$. The interaction gives rise to a quasi-regular evolution of the atomic inversion, unlike the case of one phonon resonance. This can be used for several purposes, among them, to add excitations to the vibrational state. In Fig. 8, it can be seen that if initially the ion is in its excited state $|e\rangle$, after an interaction time $\tau = \pi/\epsilon$ the ion ends up in its ground state $|g\rangle$, giving all its energy to the vibrational state by adding two vibrational quanta. Moreover, the effect of having the ion in its excited state and after an interaction time having it in the ground state is shared by all vibrational states, not only when it is prepared in a coherent state. To illustrate this fact, we show in Fig. 9 the atomic inversion for a thermal distribution

$$\rho(0) = \sum_{n=0}^{\infty} \frac{\bar{n}^n}{(\bar{n}+1)^{n+1}} |n\rangle\langle n|, \tag{121}$$

with $\bar{n}$ the average number of thermal phonons.
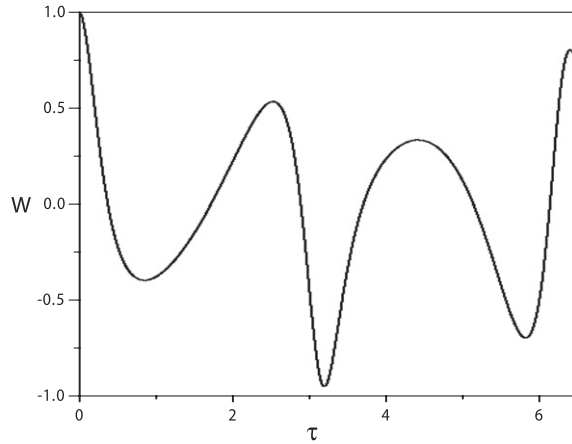
Fig. 9. Plot of the atomic inversion, $W(t) = P_2 - P_1$, the probability to find the ion in its excited state minus the probability to find it in the ground state, for an ion initially in its excited state and the vibrational state in a thermal distribution with $\bar{n} = 2$.

Consider again the initial state

$$|\Psi(0)\rangle = |\alpha\rangle|e\rangle. \tag{122}$$

Combining Eqs. (117) and (121), and using a compact operator representation of the Jaynes–Cummings dynamics, we arrive at

$$|\Psi(t)\rangle = \cos\left(\epsilon t \sqrt{\hat{a}^2(\hat{a}^\dagger)^2}\right)|\alpha\rangle|e\rangle - i(\hat{V}^\dagger)^2 \sin\left(\epsilon t \sqrt{\hat{a}^2(\hat{a}^\dagger)^2}\right)|\alpha\rangle|g\rangle. \tag{123}$$

In order to derive illustrative analytical results, in the following we will apply the approximation

$$\sqrt{\hat{a}^2(\hat{a}^\dagger)^2} \approx \hat{n} + \frac{3}{2}; \tag{124}$$

although this approximation represents a Taylor-series expansion for large eigenvalues n of the operator $\hat{n}$, the error is already small for small n-values. For example, for $n = 1$ the relative error is only 0.02.

Based on this approximation, one may simplify Eq. (123) as

$$|\Psi(t)\rangle \approx \cos[\lambda t(\hat{n} + 3/2)]|\alpha\rangle|2\rangle - i(\hat{V}^\dagger)^2 \sin[\lambda t(\hat{n} + 3/2)]|\alpha\rangle|1\rangle. \tag{125}$$

Choosing a particular interaction time $t = \tau$, according to

$$\tau = \pi/\lambda, \tag{126}$$

we obtain for the vibrational state vector

$$|\Psi_+^{(1)}(\tau)\rangle_v \approx i(\hat{V}^\dagger)^2| - \alpha\rangle, \tag{127}$$

where we have introduced the subscript "v" (vibrational) to note that we are not taking into account anymore the state $|g\rangle$. Moreover, the subscript "+" and the superscript "(k)" are used to indicate the process of adding (two) vibrational quanta and the number of such interactions, respectively.

The quantum state (127) may serve as the initial state for a second interaction with an ion that is prepared in the same manner as the first one. For the same interaction time, $t = \tau$, after the second interaction (that is completed at time 2τ), the vibrational state is

$$|\Psi_+^{(2)}(\tau)\rangle_v = -(\hat{V}^\dagger)^4|\alpha\rangle. \tag{128}$$

By repeating the process k times, one finally obtains for the quantum state, at the time t_k, after completing k interactions,

$$|\Psi_+^{(k)}(\tau)\rangle_v = i^k(\hat{V}^\dagger)^{2k}|(-1)^k\alpha\rangle. \tag{129}$$

After many interactions, the state $|\Psi_+^{(k)}(\tau)\rangle_v$ exhibits a strong sub-Poissonian character, because while one is adding two excitations per interaction, at the same time one is keeping the width of the distribution constant.

The excitation distribution $P_n^{(k)}$, after k interactions, is easily found to be related to the number statistics $P_n^{(0)}$ of the initial state $|\alpha\rangle$ via

$$P_n^{(k)} = P_{n-2k}^{(0)}. \tag{130}$$

This result clearly shows that the number statistics is only shifted but retains its form.
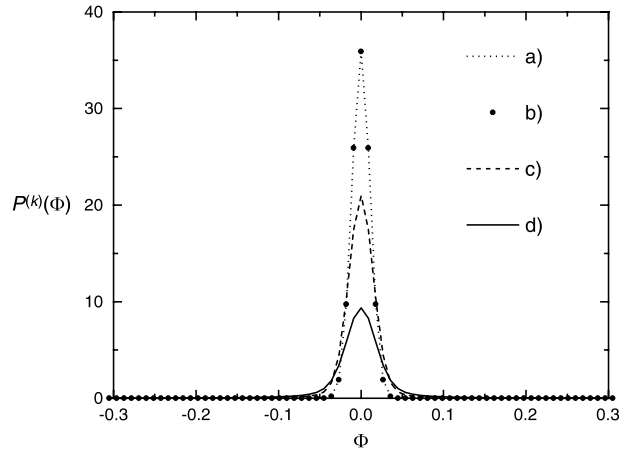
Fig. 10. Subtracted phase distribution for an initial coherent state $\alpha = 45$ and (a) $k = 0$, (b) $k = 900$, (c) $k = 1000$ and (d) $k = 1012$.

One way of studying the properties of the states being generated is through the Mandel Q-parameter [52], which is defined by

$$Q = \frac{\langle \hat{n}^2 \rangle - \langle \hat{n} \rangle^2}{\langle \hat{n} \rangle} - 1, \tag{131}$$

and where

$$\text{if } Q \begin{cases} > 0, & \text{super Poissonian distribution} \\ = 0, & \text{Poissonian distribution (coherent state)} \\ < 0, & \text{sub-Poissonian} \\ = -1, & \text{number state.} \end{cases} \tag{132}$$

In this case the Mandel Q-parameter is given by

$$Q = \frac{|\alpha|^2}{|\alpha|^2 + 2k} - 1, \tag{133}$$

and as the number of interactions increases, the Mandel Q-parameter approaches the value -1; i.e., the state acquires maximum sub-Poissonian character. The sub-Poissonian effect of the vibrational wave function becomes more significant with increasing number of interactions.

5.2. Subtracting vibrational quanta

It is straightforward to show that, opposite to the case in which we add two phonons per interaction by initially having the ion in its excited state, two phonons may be removed per interaction by initially having the ion in its ground state. We therefore expect that instead of squeezing the phonon number distribution (giving a sub-Poissonian character to the distribution), in the case in which we subtract phonons, it should be broadened; however, the conjugate variable to the number operator, i.e., the phase operator [49] should have less fluctuations; a squeezing of the phase distribution then will happen. It is not difficult to show that the phonon distribution when we subtract two phonons per interaction will be given by [12]

$$P_n^{(k)} = P_{n+2k}^{(0)}, \tag{134}$$

from which we can calculate the phase distribution plotted in Fig. 10 for several number of interactions.

5.3. Filtering specific superpositions of number states

If instead of one laser, we assume two lasers driving the ion, the first tuned to the jth lower sideband and the second tuned to the mth lower sideband, we may write $E^{(-)}(\hat{x}, t)$ as

$$E^{(-)}(\hat{x}, t) = E_j e^{-i(k_j \hat{x} - \omega_{21} + j\nu)t} + E_m e^{-i(k_m \hat{x} - \omega_{21} + m\nu)t}, \tag{135}$$

where if $m = 0$, it would correspond to the driving field being on resonance with the electronic transition. The position operator $\hat{x}$ may be written as before,

$$k_s \hat{x} = \eta_s (\hat{a} + \hat{a}^\dagger),$$ (136)

where k_s, $s = j$, m are the wave vectors of the driving fields and

$$\eta_s = 2\pi \frac{\sqrt{\langle 0 | \Delta \hat{x}^2 | 0 \rangle}}{\lambda_s}$$ (137)

are the Lamb-Dicke parameters with $s = j$, m.

In the resolved sideband limit, the vibrational frequency ν is much larger than other characteristic frequencies, and the interaction of the ion with the two lasers can be treated separately using a nonlinear Hamiltonian [16]. The Hamiltonian (106) in the interaction picture can then be written as

$$\hat{H}_I = \sigma_+ \left[\Omega_j e^{-\frac{\eta_j^2}{2}} \frac{\hat{n}!(i\eta)^j}{(\hat{n}+j)!} L_{\hat{n}}^{(j)}(\eta_j^2) \hat{a}^j + \Omega_m e^{-\frac{\eta_m^2}{2}} \frac{\hat{n}!(i\eta)^m}{(\hat{n}+m)!} L_{\hat{n}}^{(m)}(\eta_m^2) \hat{a}^m \right] + \text{H.C.},$$ (138)

where $L_{\hat{n}}^{(k)}(\eta_k^2)$ are the operator-valued associated Laguerre polynomials, the Ω's are the Rabi frequencies and $\hat{n} = \hat{a}^\dagger \hat{a}$. The master equation which describes this system can be written as

$$\frac{\partial \hat{\rho}}{\partial t} = -i[\hat{H}_I, \hat{\rho}] + \frac{\Gamma}{2} \left(2\sigma_+ \hat{\tilde{\rho}} \sigma_- - \sigma_z \hat{\rho} - \hat{\rho} \sigma_z \right)$$ (139)

where the last term describes spontaneous emission with energy relaxation rate Γ, and

$$\hat{\tilde{\rho}} = \frac{1}{2} \int_{-1}^{1} ds W(s) e^{is\eta_E \hat{x}} \hat{\rho} e^{-is\eta_E \hat{x}}$$ (140)

accounts for changes of the vibrational energy because of spontaneous emission. Here η_E is the Lamb-Dicke parameter corresponding to the field (135) and $W(s)$ is the angular distribution of spontaneous emission [16].

The steady-state solution to Eq. (139) is obtained by setting $\partial \hat{\rho} / \partial t = 0$, and may be written as

$$\hat{\rho}_s = |\psi_s\rangle |g\rangle \langle \psi_s| \langle g|,$$ (141)

where $|g\rangle$ is the electronic ground state and $|\psi_s\rangle$ is the vibrational steady-state of the ion, given by

$$\left[\Omega_j e^{-\eta_j^2/2} \frac{\hat{n}!(i\eta_j)^j}{(\hat{n}+j)!} L_{\hat{n}}^{(j)}(\eta_j^2) \hat{a}^j + \Omega_m e^{-\eta_k^2/2} \frac{\hat{n}!(i\eta_m)^m}{(\hat{n}+m)!} L_{\hat{n}}^{(m)}(\eta_m^2) \hat{a}^m \right] |\psi_s\rangle = 0.$$ (142)

For simplicity, we will concentrate in the $j = 1$ and $m = 0$ case (single number state spacing) for which Eq. (142) is written as

$$\left[i\Omega_1 \eta_1 e^{-\eta_1^2/2} \frac{L_{\hat{n}}^{(1)}(\eta_1^2)}{\hat{n}+1} \hat{a} + \Omega_0 e^{-\eta_0^2/2} L_{\hat{n}}(\eta_0^2) \right] |\psi_s\rangle = 0.$$ (143)

Note that $\hat{H}_I |1\rangle |\psi_s\rangle = 0$, so that ion and laser have stopped to interact, which occurs when the ion stops to fluoresce. For the $j = 1$ and $k = 0$ case, and assuming $L_k^{(1)}(\eta_1^2) \neq 0$ and $L_k(\eta_0^2) \neq 0$ for all k, one generates nonlinear coherent states [14]. However, by setting a value to one of the Lamb-Dicke parameters such that, for instance,

$$L_q(\eta_0^2) = 0,$$ (144)

for some integer q, we obtain that, by writing $|\psi_s\rangle$ in the number state representation,

$$|\psi_s(\eta_0)\rangle = \frac{1}{N_0} \sum_{n=0}^{q} C_n^{(0)} |n\rangle,$$ (145)

(the argument of ψ_s denotes the condition we apply; i.e., in Eq. (145), the condition is on η_0) where

$$C_n^{(0)} = \left(-\frac{\Omega_0 e^{-\eta_0^2/2}}{\Omega_1 e^{-\eta_1^2/2}} \right)^n (n!)^{1/2} \prod_{m=0}^{n-1} \frac{L_m(\eta_0^2)}{L_m^1(\eta_1^2)},$$

$$C_0^{(0)} = 1,$$ (146)

and

$$N_0^2 = \sum_{n=0}^{q} |C_n^{(0)}|^2 \tag{147}$$

is the normalization constant.

If instead of condition (144), we choose

$$L_p^{(1)}(\eta_1^2) = 0, \tag{148}$$

we obtain the wave function

$$|\psi_s(\eta_1)\rangle = \frac{1}{N_1} \sum_{n=p+1}^{\infty} C_n^{(1)} |n\rangle, \tag{149}$$

where now

$$C_n^{(1)} = \left(-\frac{\Omega_0 e^{-\eta_0^2/2}}{\Omega_1 e^{-\eta_1^2/2}} \right)^{n-p-1} \sqrt{\frac{n!}{(p+1)!}} \prod_{m=p+1}^{n-1} \frac{L_m(\eta_0^2)}{L_m^1(\eta_1^2)},$$

$$C_{p+1}^{(1)} = 1, \tag{150}$$

and

$$N_1^2 = \sum_{n=p+1}^{\infty} |C_n^{(1)}|^2. \tag{151}$$

Combining both conditions, (144) and (148), one would obtain for $q > p$,

$$|\psi_s(\eta_0, \eta_1)\rangle = \frac{1}{N_{01}} \sum_{n=p+1}^{q} C_n^{(1)} |n\rangle, \tag{152}$$

with

$$N_{01}^2 = \sum_{n=p+1}^{q} |C_n^{(1)}|^2. \tag{153}$$

In this way, by setting the conditions (144), (148) or both, we can engineer states in the following three zones of the Hilbert space: (a) from $|0\rangle$ to $|q\rangle$, (b) from $|p+1\rangle$ to $|\infty\rangle$, or (c) from $|p+1\rangle$ to $|q\rangle$. In the later case, by setting $q = p+1$, generation of the number state $|q\rangle$ is achieved.

We should remark that by selecting further apart sidebands one would obtain a different spacing in Eqs. (145), (149) and (152). For instance, by choosing $j = 2$ and $k = 0$ one would obtain only even or odd number states in those equations (depending in this case on initial conditions, and $W(s)$, the angular distribution of spontaneous emission). Also, it should be noticed that one can use the parameters $j = m+1$ and $k = m$ (with $m \neq 0$) (in the single number state spacing case) to extend the possibilities of choosing Lamb-Dicke parameters. Lamb-Dicke parameters of the order of one (or less) are needed (for conditions (10) and (12)), which can be achieved by varying the geometry of the lasers. For example, by setting $\eta_0 = 1$, we have $L_1(\eta_0^2 = 1) = 0$, and therefore we obtain the qubit

$$|\psi_s(\eta_0 = 1)\rangle = \frac{1}{\sqrt{1 + |\frac{\Omega_0}{\Omega_1}|^2 e^{\eta_1^2 - 1}}} \left(|0\rangle - \frac{\Omega_0 e^{-1/2}}{\Omega_1 e^{-\eta_1^2/2}} |1\rangle \right), \tag{154}$$

where by changing the Rabi frequencies, one has control of the amplitudes. Finally, note that we could have also chosen to drive the qth upper sideband instead of the kth lower sideband in Eq. (135) with basically the same results.

5.4. N00N states

Nonclassical states have attracted a great deal of attention in recent years, among them are (a) macroscopic quantum superpositions of quasiclassical coherent states with different mean phases or amplitudes [53,54], (b) squeezed states [55,31], (c) the particularly important limit of extreme squeezing; i.e., Fock or number states, and more recently, (d) nonclassical states of combined photon pairs also called N00N states [56,57]. It is well known that these multiphoton entangled states can be used to obtain high-precision phase measurements, becoming more and more advantageous as the number of photons grows. Many applications in quantum imaging, quantum information and quantum metrology [58] depend on the availability of entangled photon pairs because entanglement is a distinctive feature of quantum mechanics
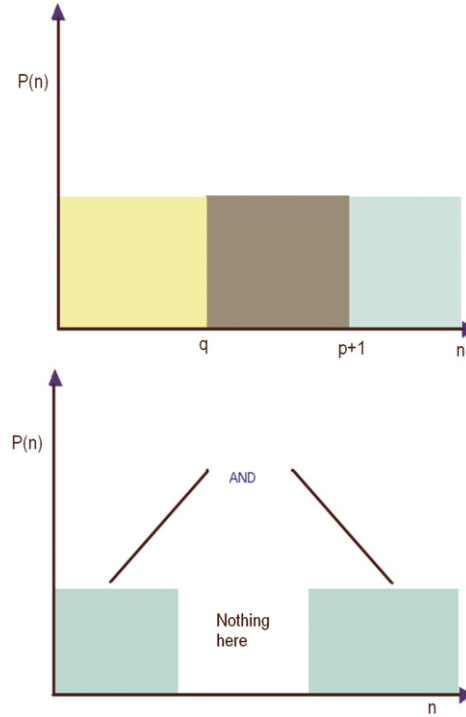
Fig. 11. Possible situations we can have if we filter number states with the proposals of this section.

that lies at the core of many new applications. These maximally path-entangled multiphoton states may be written in the form

$$|N00N\rangle_{a,b} = \frac{1}{\sqrt{2}} \left(|N\rangle_a |0\rangle_b + |0\rangle_a |N\rangle_b \right). \tag{155}$$

It has been pointed out that N00N states manifest unique coherence properties by showing that they exhibit a periodic transition between spatially bunched and antibunched states when undergo Bloch oscillations. The period of the bunching/antibunching oscillation is N times faster than the period of the oscillation of the photon density [59].

The greatest N for which N00N states have been produced is N = 5 [56]. Most schemes to generate this class of states are either for optical [56,57] or microwave [60] fields. In this contribution, we would like to analyze the possibility to generate them in ions [39–43], i.e., N00N states of their vibrational motion. We will show that they may be generated with N = 8. (See Fig. 11.)

5.4.1. Ion vibrating in two dimensions

We consider an ion in a two-dimensional Paul trap [61], and we assume that the ion is driven by a plane wave

$$E^{(-)}(\hat{x}, \hat{y}, t) = E_0 e^{-i(k_x \hat{x} + k_y \hat{y} + \omega)t}, \tag{156}$$

with $k_j, j = x, y$ the wavevectors of the driving field. The Hamiltonian has the form

$$H = \nu_x \hat{a}_x^\dagger \hat{a}_x + \nu_y \hat{a}_y^\dagger \hat{a}_y + \frac{\omega_{21}}{2} \hat{\sigma}_z + \Omega_x \left\{ e^{-i\left[\eta_x\left(\hat{a}_x + \hat{a}_x^\dagger\right) + \omega t\right]} \hat{\sigma}_+ + \text{H.C.} \right\} + \Omega_y \left\{ e^{-i\left[\eta_y\left(\hat{a}_y + \hat{a}_y^\dagger\right) + \omega t\right]} \hat{\sigma}_+ + \text{H.C.} \right\}. \tag{157}$$

where we have defined the Lamb-Dicke parameters

$$\eta_x = 2\pi \frac{\sqrt{{}_x\langle 0| \Delta \hat{x}^2 |0\rangle_x}}{\lambda_x}, \qquad \eta_y = 2\pi \frac{\sqrt{{}_y\langle 0| \Delta \hat{y}^2 |0\rangle_y}}{\lambda_y}, \tag{158}$$

and redefined the ladder operators according to

$$k_x \hat{x} = \eta_x (a_x + a_x^\dagger), \qquad k_{\text{and}} \hat{y} = \eta_y (a_y + a_y^\dagger). \tag{159}$$

In the resolved sideband limit, the vibrational frequencies ν_x and ν_y are much larger than other characteristic frequencies and the interaction of the ion with the two lasers can be treated separately using a nonlinear Hamiltonian [16,17].

We consider that the ion is trapped in the *x*-axis, i.e., $\Omega_x \neq 0$ and $\Omega_y = 0$; then

$$H_x = \nu_x \hat{a}_x^\dagger \hat{a}_x + \frac{\omega_{21}}{2} \hat{\sigma}_z + \Omega_x \left\{ e^{-i\left[\eta_x\left(\hat{a}_x + \hat{a}_x^\dagger\right) + \omega t\right]} \hat{\sigma}_+ + \text{H.C.} \right\}. \tag{160}$$

We write $\omega_{21} = \omega + \delta$, where δ is the detuning, to obtain

$$H_x = \nu_x \hat{a}_x^\dagger \hat{a}_x + \frac{(\omega + \delta)}{2} \hat{\sigma}_z + \Omega_x \left\{ e^{-i\left[\eta_x\left(\hat{a}_x + \hat{a}_x^\dagger\right) + \omega t\right]} \hat{\sigma}_+ + \text{H.C.} \right\}. \tag{161}$$

We transform the Hamiltonian to a frame rotating at ω frequency by means of the transformation

$$T = e^{-i\frac{\omega t}{2}\sigma_z}, \tag{162}$$

and we get

$$H_x = \nu_x \hat{a}_x^\dagger \hat{a}_x + \frac{\delta}{2} \hat{\sigma}_z + \Omega_x \left\{ e^{-i\left[\eta_x\left(\hat{a}_x + \hat{a}_x^\dagger\right)\right]} \hat{\sigma}_+ + e^{i\left[\eta_x\left(\hat{a}_x + \hat{a}_x^\dagger\right)\right]} \hat{\sigma}_- \right\}. \tag{163}$$

Using the Baker–Hausdorff formula [48], and expanding the exponentials in Taylor series, we cast the Hamiltonian to

$$H_x = \nu_x \hat{a}_x^\dagger \hat{a}_x + \frac{\delta}{2} \hat{\sigma}_z + \Omega_x \left[e^{-\frac{\eta_x^2}{2}} \sum_{n,m} \frac{(-i\eta_x)^n}{n!} \frac{(-i\eta_x)^m}{m!} \hat{a}_x^{\dagger n} \hat{a}_x^m \hat{\sigma}_+ + \text{H.C.} \right]. \tag{164}$$

Going now to the interaction picture,

$$H_{Ix} = \Omega_x \left[e^{-\frac{\eta_x^2}{2}} \sum_{n,m} \frac{(-i\eta_x)^n}{n!} \frac{(-i\eta_x)^m}{m!} \hat{a}_x^{\dagger n} \hat{a}_x^m \hat{\sigma}_+ e^{i\nu_x t(n-m+k)} + \text{H.C.} \right]. \tag{165}$$

We consider now the low-intensity regime; i.e., $\Omega_x \ll \nu_x$, and we apply the rotating wave approximation, to get

$$H_{Ix} = \Omega_x \left[e^{-\frac{\eta_x^2}{2}} (-i\eta_x)^k \sum_{n=0}^{\infty} \frac{(-\eta_x)^{2n}}{n!\,(k+n)!} \hat{a}_x^{\dagger n} \hat{a}_x^{k+n} \hat{\sigma}_+ + \text{H.C.} \right], \tag{166}$$

by substituting $\hat{a}_x^{\dagger n} \hat{a}_x^n = \frac{\hat{n}!}{(\hat{n}-n)!}$, multiplying by $\frac{(\hat{n}+k)!}{(\hat{n}+k)!}$, and rearranging terms

$$H_{Ix} = \Omega_x \left[e^{-\frac{\eta_x^2}{2}} (-i\eta_x)^k \frac{\hat{n}!}{(\hat{n}+k)!} L_{\hat{n}}^k \left(\eta_x^2\right) \hat{a}_x^k \hat{\sigma}_+ + \text{H.C.} \right], \tag{167}$$

where we have identified $L_{\hat{n}}^k \left(\eta_x^2\right) = \sum_{n=0}^{\hat{n}} \frac{(-1)^n \left(\eta_x^2\right)^n}{n!} \frac{(\hat{n}+k)!}{(n+k)!(\hat{n}-n)!}$, with the associated Laguerre polynomials; so that finally

$$H_{Ix} = \Omega_x \left(f_x^k \left(\hat{n}\right) \hat{a}_x^k \hat{\sigma}_+ + \hat{a}_x^{\dagger k} f_x^{*k} \left(\hat{n}\right) \hat{\sigma}_- \right), \tag{168}$$

where

$$f_x^k \left(\hat{n}\right) = e^{-\frac{\eta_x^2}{2}} (-i\eta_x)^k \frac{\hat{n}!}{(\hat{n}+k)!} L_{\hat{n}}^k \left(\eta_x^2\right). \tag{169}$$

We write the Hamiltonian, given by expression (168), in the following matrix form

$$H_{Ix} = \begin{pmatrix} 0 & \Omega_x f_x^k \left(\hat{n}\right) \hat{a}_x^k \\ \Omega_x \hat{a}_x^{\dagger k} f_x^{*k} \left(\hat{n}\right) & 0 \end{pmatrix}, \tag{170}$$

which, by using the Susskind–Glogower phase operator [62], we can be written as

$$H_{Ix} = \begin{pmatrix} 1 & 0 \\ 0 & \hat{V}_x^{\dagger k} \end{pmatrix} H_{1x} \begin{pmatrix} 1 & 0 \\ 0 & \hat{V}_x^k \end{pmatrix} \tag{171}$$

where we have introduced and defined

$$H_{1x} = \begin{pmatrix} 0 & \Omega_x f_x^k \left(\hat{n}\right) \sqrt{\hat{a}_x^k \hat{a}_x^{\dagger k}} \\ \Omega_x f_x^{*k} \left(\hat{n}\right) \sqrt{\hat{a}_x^k \hat{a}_x^{\dagger k}} & 0 \end{pmatrix}. \tag{172}$$

The evolution operator for this last transformed Hamiltonian, $U_{1x} = e^{-iH_{1x}t}$, may be calculated easily. For this we need

$$H_{1x}^{2m} = \begin{pmatrix} \Omega_x^{2m} \left| f_x^k\left(\hat{n}\right)\right|^{2m} \left(\sqrt{\hat{a}_x^k \hat{a}_x^{\dagger k}}\right)^{2m} & 0 \\ 0 & \Omega_x^{2m} \left| f_x^k\left(\hat{n}\right)\right|^{2m} \left(\sqrt{\hat{a}_x^k \hat{a}_x^{\dagger k}}\right)^{2m} \end{pmatrix}, \tag{173}$$

and

$$H_{1x}^{2m+1} = \begin{pmatrix} 0 & \Omega_x^{2m+1} \dfrac{\left| f_x^k\left(\hat{n}\right)\right|^{2m+1} f_x^{*k}\left(\hat{n}\right)}{\left| f_x^k\left(\hat{n}\right)\right|} \left(\sqrt{\hat{a}_x^k \hat{a}_x^{\dagger k}}\right)^{2m+1} \\ \Omega_x^{2m+1} \dfrac{\left| f_x^k\left(\hat{n}\right)\right|^{2m+1} f_x^{*k}\left(\hat{n}\right)}{\left| f_x^k\left(\hat{n}\right)\right|} \left(\sqrt{\hat{a}_x^k \hat{a}_x^{\dagger k}}\right)^{2m+1} & 0 \end{pmatrix}. \tag{174}$$

Then

$$U_{1x}(t) = \sum_m \frac{(-it)^{2m}}{(2m)!} H_{1x}^{2m} + \sum_m \frac{(-it)^{2m+1}}{(2m+1)!} H_{1x}^{2m+1}, \tag{175}$$

and therefore

$$U_{Ix}(t) = \begin{pmatrix} \cos\left(\Omega_x t \left| f_x^k\left(\hat{n}\right)\right| \sqrt{\hat{a}_x^k \hat{a}_x^{\dagger k}}\right) & -i(-i)^k \sin\left(\Omega_x t \left| f_x^k\left(\hat{n}\right)\right| \sqrt{\hat{a}_x^k \hat{a}_x^{\dagger k}}\right) \hat{V}_x^k \\ -i\hat{V}_x^{\dagger k} (i)^k \sin\left(\Omega_x t \left| f_x^k\left(\hat{n}\right)\right| \sqrt{\hat{a}_x^k \hat{a}_x^{\dagger k}}\right) & \hat{V}_x^{\dagger k} \cos\left(\Omega_x t \left| f_x^k\left(\hat{n}\right)\right| \sqrt{\hat{a}_x^k \hat{a}_x^{\dagger k}}\right) \hat{V}_x^k \end{pmatrix}. \tag{176}$$

Finally, as $\sqrt{\hat{a}_x^k \hat{a}_x^{\dagger k}} = \sqrt{\frac{(\hat{n}+k)!}{\hat{n}!}}$, we can write

$$U_{Ix}(t) = \begin{pmatrix} \cos\left[\Omega_x t \left| f_x^k\left(\hat{n}\right)\right| \sqrt{\dfrac{(\hat{n}+k)!}{\hat{n}!}}\right] & (-i)^{k+1} \sin\left[\Omega_x t \left| f_x^k\left(\hat{n}\right)\right| \sqrt{\dfrac{(\hat{n}+k)!}{\hat{n}!}}\right] \hat{V}_x^k \\ -(i)^{k+1} \hat{V}_x^{\dagger k} \sin\left[\Omega_x t \left| f_x^k\left(\hat{n}\right)\right| \sqrt{\dfrac{(\hat{n}+k)!}{\hat{n}!}}\right] & \hat{V}_x^{\dagger k} \cos\left[\Omega_x t \left| f_x^k\left(\hat{n}\right)\right| \sqrt{\dfrac{(\hat{n}+k)!}{\hat{n}!}}\right] \hat{V}_x^k \end{pmatrix}. \tag{177}$$

Now, we consider as initial state of the ion a number state $|n\rangle$ for the vibrational motion and the excited state $|e\rangle$ for the internal states; i.e.,

$$|\psi(0)\rangle = \begin{pmatrix} |n\rangle \\ 0 \end{pmatrix}. \tag{178}$$

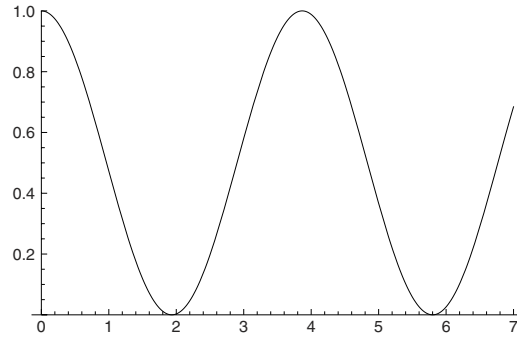The probability, after the time t, of finding the ion in its internal excited state is then

$$P_e(t) = \sum_{m=0}^{\infty} \langle e|\langle m|\psi(t)\rangle \langle \psi(t)|m\rangle|e\rangle = \cos^2\left(\Omega_x t \left| f_x^k(n)\right| \sqrt{\frac{(\hat{n}+k)!}{\hat{n}!}}\right). \tag{179}$$

It is clear that after a time

$$t_0 = \frac{\pi}{2} \frac{1}{\Omega_x \left| f_x^k(n)\right|} \sqrt{\frac{n!}{(n+k)!}} \tag{180}$$

the probability to find the ion in its internal excited state is 0. So at that time the ion is in its internal ground state with probability 1. This situation is obviously repeated periodically; every $2j+1$, $j = 0, 1, 2, \ldots$ times t_0, the ion will be in its ground state. We plot in Fig. 12, the probability for the case when $k = 4$ and the ionic vibration is initially in a number state with $n = 4$. As can be seen from Hamiltonian (168), when the probability of finding the ion in the excited state goes to zero, the ion is giving four phonons to the vibrational motion. Now, if we consider the ion initially in its ground state, the probability to find it in the ground state at the same time t_0 is also zero. In this case the ion removes four phonons of the vibrational motion.

If we consider now that the ion is trapped in the y-axis; i.e., $\Omega_y \neq 0$ and $\Omega_x = 0$, we get exactly the same expressions and the same results with the variable y instead of x.

Fig. 12. The probability, after the time τ, of finding the ion in its internal excited state when initially the ion was in its excited state and the ionic vibration was a number state with $n = 4$ and $\eta_x = 0.1$.

5.4.2. Generation of N00N states

By starting with the ion in the excited state and the vibrational state in the vacuum state, i.e., $|0\rangle_x|0\rangle_y$, if we set $\eta_y = 0$, after the time τ_p when the probability to find the ion in its excited state is zero (meaning that the ion, by passing from its excited to its ground state, gives 4 phonons to the vibrational motion), we can generate the state $|4\rangle_x|0\rangle_y$. Repeating this procedure (with the ion reset again to the excited state, via a rotation), but now with $\eta_x = 0$, four phonons are added to the y-vibrational motion, generating the two-dimensional state $|4\rangle_x|4\rangle_y$.

Therefore, if we consider the ion initially in a superposition of ground and excited states, and the $|4\rangle_x|4\rangle_y$ vibrational state; i.e.,

$$|\psi_{init}\rangle = \frac{1}{\sqrt{2}}(|e\rangle + |g\rangle)|4\rangle_x|4\rangle_y, \tag{181}$$

for $\eta_y = 0$ and t_0, the state generated is

$$|\psi_{\eta_y=0}\rangle = \frac{i}{\sqrt{2}}(|e\rangle|0\rangle_x + |g\rangle|8\rangle_x)|4\rangle_y. \tag{182}$$

Now, we consider this state as initial state for the next interaction with $\eta_x = 0$ and still the interaction time τ_p, to produce

$$|\psi_{\eta_x=0}\rangle = -\frac{1}{\sqrt{2}}(|e\rangle|0\rangle_x|8\rangle_y + |g\rangle|8\rangle_x|0\rangle_y). \tag{183}$$

Next, the ion is rotated via a classical field (an on-resonance interaction) such that the state

$$|\psi_R\rangle = -\frac{1}{2}\left[|e\rangle(|0\rangle_x|8\rangle_y - |8\rangle_x|0\rangle_y) + |g\rangle(|0\rangle_x|8\rangle_y + |8\rangle_x|0\rangle_y)\right] \tag{184}$$

is obtained. Finally by measuring the ion in its excited state we produce the N00N state

$$|N00N_e\rangle = \frac{1}{\sqrt{2}}(|0\rangle_x|8\rangle_y - |8\rangle_x|0\rangle_y), \tag{185}$$

and if the ion is measured in the ground state, also a N00N state is produced:

$$|N00N_g\rangle = \frac{1}{\sqrt{2}}(|0\rangle_x|8\rangle_y + |8\rangle_x|0\rangle_y). \tag{186}$$

5.5. Measuring squeezing

In this section, we have shown how to generate nonclassical states of the vibrational motion of the ion. The question arises: Can we measure nonclassical features in this interaction? Here we propose a method to measure squeezing. In order to achieve this we need to be able to measure quantities like

$$\langle \hat{X}\rangle = \langle \hat{a}\rangle + \text{c.c.}, \qquad \langle \hat{X}^2\rangle = \langle \hat{a}^2\rangle + \langle[\hat{a}^\dagger]^2\rangle + 2\langle \hat{n}\rangle + 1. \tag{187}$$

Below we will show how it is possible to measure such quantities by utilizing an atom as a measuring device. Consider the Hamiltonian (109), which in matrix form may be written as

$$H = -i\eta\Omega(\hat{a}^\dagger\hat{\sigma}_- - \hat{\sigma}_+\hat{a}) = -i\eta\Omega\begin{pmatrix} 0 & -\hat{a} \\ \hat{a}^\dagger & 0 \end{pmatrix}. \tag{188}$$

We can re-write Hamiltonian (188) with the help of Susskind–Glogower operators [62] as

$$H = -i\eta\Omega R \begin{pmatrix} 0 & -\sqrt{\hat{n}+1} \\ \sqrt{\hat{n}+1} & 0 \end{pmatrix} R^{\dagger}, \tag{189}$$

where

$$R = \begin{pmatrix} 1 & 0 \\ 0 & \hat{V}^{\dagger} \end{pmatrix} \tag{190}$$

with $\hat{V} = \frac{1}{\sqrt{\hat{n}+1}}\hat{a}$. Note that $R^{\dagger}R = 1$, but $RR^{\dagger} \neq 1$. This allows us to write the evolution operator as

$$U(t) = R \begin{pmatrix} \cos(\eta\Omega t\sqrt{\hat{n}+1}) & -\sin(\eta\Omega t\sqrt{\hat{n}+1}) \\ \sin(\eta\Omega t\sqrt{\hat{n}+1}) & \cos(\eta\Omega t\sqrt{\hat{n}+1}) \end{pmatrix} R^{\dagger}. \tag{191}$$

We are neglecting a term $|0\rangle\langle 0|$ in the above evolution operator (in the element "2, 2"), that however will not affect the measurement of squeezing as we will consider the ion in the excited state. We consider the vibrational wave function in an unknown state, such that the initial state of the system is $|\psi(0)\rangle = |e\rangle|\psi_v(0)\rangle$; the average of the operator $\hat{\sigma}_+$ is given by

$$\langle\hat{\sigma}_+\rangle = \langle\psi_v(0)| \cos\left(\eta\Omega t\sqrt{\hat{n}+1}\right)\hat{V}^{\dagger}\sin\left(\eta\Omega t\sqrt{\hat{n}+1}\right)|\psi_v(0)\rangle$$

$$= \frac{1}{2}\langle\psi_v(0)|\hat{V}^{\dagger}\left(\sin[\eta\Omega t\hat{\Delta}_+(\hat{n})] - \sin[\eta\Omega t\hat{\Delta}_-(\hat{n})]\right)|\psi_v(0)\rangle, \tag{192}$$

where

$$\hat{\Delta}_+(\hat{n}) = \sqrt{\hat{n}+2} + \sqrt{\hat{n}+1}, \qquad \hat{\Delta}_-(\hat{n}) = \sqrt{\hat{n}+2} - \sqrt{\hat{n}+1}. \tag{193}$$

By integrating (193) by using a Fresnel integral [51]

$$\int_0^{\infty} dT T \sin(T^2/A) \sin(BT) = \frac{AB}{4}\sqrt{\frac{\pi A}{2}}\left(\cos\frac{AB^2}{4} + \sin\frac{AB^2}{4}\right), \tag{194}$$

such that (with $\eta\Omega t = T$)

$$\int_0^{\infty} dT T \sin(T^2/A)\langle\hat{\sigma}_+\rangle = -\frac{i}{2}\langle\psi_F(0)|\hat{V}^{\dagger}(\hat{\gamma}_1 - \hat{\gamma}_2)|\psi_F(0)\rangle \tag{195}$$

with

$$\hat{\gamma}_1^{(1)} = \frac{A\hat{\Delta}_+(\hat{n})}{4}\sqrt{\frac{\pi A}{2}}\left(\cos\left[\frac{A\hat{\Delta}_+^2(\hat{n})}{4}\right] + \sin\left[\frac{A\hat{\Delta}_+^2(\hat{n})}{4}\right]\right) \tag{196}$$

and

$$\hat{\gamma}_2^{(1)} = \frac{A\hat{\Delta}_-(\hat{n})}{4}\sqrt{\frac{\pi A}{2}}\left(\cos\left[\frac{A\hat{\Delta}_-^2(\hat{n})}{4}\right] + \sin\left[\frac{A\hat{\Delta}_-^2(\hat{n})}{4}\right]\right). \tag{197}$$

Now we use the approximation [63,64] $\sqrt{(\hat{n}+2)(\hat{n}+1)} \approx \hat{n}+3/2$ that is valid for large photon numbers; we then can write $\hat{\Delta}_+^2(\hat{n}) \approx 4\hat{n}+6$ and $\hat{\Delta}_-^2(\hat{n}) \approx 0$. By setting $A = 4\pi$, we obtain

$$\hat{\gamma}_1^{(1)} \approx \left(\sqrt{\hat{n}+2} + \sqrt{\hat{n}+1}\right)\pi \cos\left[(4\hat{n}+6)\pi\right] = \sqrt{2}\pi^2\hat{\Delta}_+(\hat{n}) \tag{198}$$

and

$$\hat{\gamma}_2^{(1)} \approx \sqrt{2}\pi^2\hat{\Delta}_-(\hat{n}), \tag{199}$$

so that the integral transform (195) becomes

$$\int_0^{\infty} dT T \sin(T^2/A)\langle\hat{\sigma}_+\rangle = \sqrt{2}\pi^2\langle\psi_v(0)|\hat{V}^{\dagger}\sqrt{\hat{n}+1}|\psi_v(0)\rangle$$

$$= \sqrt{2}\pi^2\langle\psi_v(0)|\hat{a}^{\dagger}|\psi_v(0)\rangle. \tag{200}$$

To measure $\langle\psi_F(0)|[\hat{a}^\dagger]^2|\psi_F(0)\rangle$ a two-phonon transition is necessary; in this case

$$H_2 = \lambda^{(2)}\hat{R}^2 \begin{pmatrix} 0 & \sqrt{(\hat{n}+1)(\hat{n}+2)} \\ \sqrt{(\hat{n}+1)(\hat{n}+2)} & 0 \end{pmatrix} [R^\dagger]^2, \tag{201}$$

where $\lambda^{(2)}$ is the interaction constant in the two-phonon case. One can find the evolution operator that will be given by an expression similar to (191), just changing $\sqrt{\hat{n}+1} \rightarrow \sqrt{(\hat{n}+1)(\hat{n}+2)}$, $\hat{V} \rightarrow \hat{V}^2$ and $\hat{V}^\dagger \rightarrow [\hat{V}^\dagger]^2$. It is then easy to calculate the average of $\hat{\sigma}_+^{(2)}$, which is given by

$$\langle\hat{\sigma}_+^{(2)}\rangle = -i\langle\psi_F(0)|\cos\left[\lambda^{(2)}t\sqrt{(\hat{n}+1)(\hat{n}+2)}\right][\hat{V}^\dagger]^2\sin\left[\lambda^{(2)}t\sqrt{(\hat{n}+1)(\hat{n}+2)}\right]|\psi_F(0)\rangle$$

$$= -\frac{i}{2}\langle\psi_F(0)|[\hat{V}^\dagger]^2\left(\sin[\lambda t\hat{\delta}_+(\hat{n})] - \sin[\lambda t\hat{\delta}_-(\hat{n})]\right)|\psi_F(0)\rangle \tag{202}$$

with

$$\hat{\delta}_+(\hat{n}) = \sqrt{(\hat{n}+4)(\hat{n}+3)} + \sqrt{(\hat{n}+2)(\hat{n}+1)} \approx 2\hat{n} + 5, \tag{203}$$

and

$$\hat{\delta}_-(\hat{n}) = \sqrt{(\hat{n}+4)(\hat{n}+3)} - \sqrt{(\hat{n}+2)(\hat{n}+1)} \approx 2. \tag{204}$$

Again by (Fresnel) integration of the above expression

$$\int_0^\infty dT T \sin(T^2/A)\langle\hat{\sigma}_+^{(2)}\rangle = -i4\pi^2\langle\psi_F(0)|[\hat{V}^\dagger]^2(\hat{\gamma}_1^{(2)} - \hat{\gamma}_2^{(2)})|\psi_F(0)\rangle \tag{205}$$

with

$$\hat{\gamma}_1^{(2)} = \frac{A\hat{\delta}_+(\hat{n})}{4}\sqrt{\frac{\pi A}{2}}\left(\cos\left[\frac{A\hat{\delta}_+^2(\hat{n})}{4}\right] + \sin\left[\frac{A\hat{\delta}_+^2(\hat{n})}{4}\right]\right) \tag{206}$$

and

$$\hat{\gamma}_2^{(2)} = \frac{A\hat{\delta}_-(\hat{n})}{4}\sqrt{\frac{\pi A}{2}}\left(\cos\left[\frac{A\hat{\delta}_-^2(\hat{n})}{4}\right] + \sin\left[\frac{A\hat{\delta}_-^2(\hat{n})}{4}\right]\right). \tag{207}$$

By choosing the value $A = 8\pi$, we obtain

$$\int_0^\infty dT T \sin(T^2/8\pi)\langle\hat{\sigma}_+^{(2)}\rangle = -i8\pi^4\langle\psi_F(0)|[\hat{V}^\dagger]^2\sqrt{(\hat{n}+1)(\hat{n}+1)}|\psi_F(0)\rangle$$

$$= -i8\pi^4\langle[\hat{a}^\dagger]^2\rangle. \tag{208}$$

Therefore, squeezing may be measured via this scheme.

6. Ion–laser interaction in a trap with time-dependent frequency

In this section, we study the problem of an ion trapped with a frequency that depends on time and interacting with a laser beam [65,66]. Using unitary transformations, we show that this system is equivalent to a system formed by a two level subsystem with time dependent parameters interacting with a quantized field. The procedure to build the Hamiltonian for this case is exactly the same as that in the time independent frequency case (Section 3), but we have to keep in mind that now the frequency is time dependent.

The Hamiltonian is

$$H = \frac{1}{2}\left[p^2 + \nu^2(t)x^2\right] + \frac{1}{2}\omega_{21}\sigma_z + \lambda\left[E^{(-)(x,t)}\sigma_- + \text{H.C.}\right], \tag{209}$$

and then the Schrödinger equation can be written as

$$i\frac{\partial}{\partial t}|\xi(t)\rangle = H|\xi(t)\rangle. \tag{210}$$

To solve the problem, we make the transformation

$$|\phi(t)\rangle = T_{SD}(t)|\xi(t)\rangle, \tag{211}$$

where

$$T_{SD}(t) = \exp\left\{\frac{i \ln\left[\rho(t)\sqrt{\nu_0}\right](xp + px)}{2}\right\} \exp\left[\frac{-i\dot{\rho}(t)x^2}{2\rho(t)}\right], \tag{212}$$

and we have also the Ermakov equation

$$\frac{d^2\rho}{dt^2} + \nu^2(t)\rho = \frac{1}{\rho^3}, \tag{213}$$

as an auxiliary equation. We apply the unitary transformation (212) to the Hamiltonian (209); i.e., we must calculate the expression

$$H_{SD} = i\frac{\partial T_{DS}(t)}{\partial t}T_{SD}^{\dagger}(t) + T_{SD}(t)HT_{SD}^{\dagger}(t). \tag{214}$$

We find,

$$H_{SD} = \frac{1}{2\nu_0\rho^2(t)}(p^2 + \nu_0^2 x^2) + \frac{1}{2}\omega_{21}\sigma_z + \Omega\left\{\exp\left[-i\left(k\rho(t)\sqrt{\nu_0}x^2 - \omega t\right)\right]\sigma_- + \text{H.C.}\right\}, \tag{215}$$

with $\Omega = \lambda E_0$, the Rabi frequency.

Using the Ermakov invariant, the time dependence of the trap has been factorized; the time dependence is implicit in $\rho(t)$. We now go to a frame rotating at frequency ω, by means of the unitary transformation

$$T_{\omega}(t) = \exp\left(\frac{i}{2}\omega t\sigma_z\right). \tag{216}$$

The Hamiltonian is transformed to

$$H_{\omega} = \frac{1}{2\nu_0\rho^2(t)}(p^2 + \nu_0^2 x^2) + \frac{1}{2}(\omega_{21} - \omega)\sigma_z + \Omega(t)\left\{\exp\left[-i(\hat{a} + \hat{a}^{\dagger})\eta(t)\right]\sigma_- + \text{H.C.}\right\}. \tag{217}$$

Denoting the detuning frequency between the laser and the ion by $\delta = \omega_{21} - \omega$, and the characteristic frequency of the time dependent harmonic oscillator by

$$\tilde{\omega}(t) = \frac{1}{\rho^2(t)}, \tag{218}$$

we get

$$H_{\omega} = \tilde{\omega}(t)(\hat{n} + 1/2) + \frac{\delta}{2}\sigma_z + \Omega(t)\left\{\exp\left[-i(\hat{a} + \hat{a}^{\dagger})\eta(t)\right]\sigma_- + \text{H.C.}\right\}. \tag{219}$$

The time dependent Lamb-Dicke parameter is

$$\eta(t) = \eta_0\rho(t)\sqrt{\nu_0}, \tag{220}$$

with

$$\eta_0 = k\sqrt{\frac{1}{2\nu_0}}, \tag{221}$$

where k is the wave vector of the laser beam. Comparing with the Hamiltonian (93), the Hamiltonian (219) is equivalent, but with all the parameters depending on time.

6.1. Exact linearization of the system

We call linearization of the system the process to reduce the exponent of the ladder operators $\hat{a}$ and $\hat{a}^{\dagger}$ to the first power, without using approximations. To this end, we make the transformation

$$|\phi_R\rangle = R(t)|\phi_{\omega}\rangle, \tag{222}$$

where $R(t)$ is given by

$$R(t) = \exp\left[-\frac{\pi}{4}(\sigma_+ - \sigma_-)\right]\exp\left[-i\frac{\eta(t)}{2}(\hat{a} + \hat{a}^{\dagger})\sigma_z\right]. \tag{223}$$
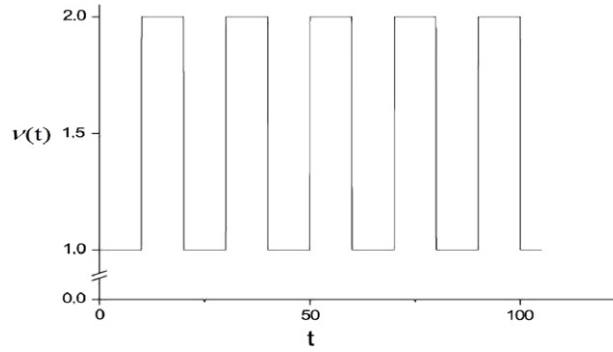
Fig. 13. Trap's time dependent frequency as a train of steps.

Transforming the Hamiltonian, we get

$$H_R = \nu_0 \hat{n} + \Omega \sigma_z + \left\{ \frac{\delta}{2} + i \left[\hat{a} \beta(t) - \hat{a}^\dagger \beta^*(t) \right] \right\} (\sigma_+ + \sigma_-) \tag{224}$$

with

$$\beta(t) = \frac{\eta(t) \tilde{\omega}}{2} - \frac{i \dot{\eta}(t)}{2}. \tag{225}$$

The term $\tilde{\omega}(t)/2$ has not been considered, because it is only a phase, and when the observable mean values are taken, it disappears.

With the transformation (223) we have achieved our goal: linearize the Hamiltonian without any type of approximation. The rotating wave approximation is not used, and this leaves open the possibility to consider different intensity regimes. No assumption has been made about the Lamb-Dicke parameter $\eta(t)$. It is also valid for any type of detuning and for any time dependence of the frequency of the trap.

It is also important to remark that we have not imposed any condition in the time dependence of the frequency of the trap; in principle, this frequency can assume any temporal form. For a Paul trap, the more general form is

$$\nu^2(t) = a - 2q \cos 2t, \tag{226}$$

and the Hamiltonian (224) is the ion–laser interaction with micromotion included. Also, this Hamiltonian gives us the freedom to consider arbitrary time dependent frequencies. For instance, if we consider a sudden change in the trap frequency, we would generate squeezed states for the vibrational wave function.

6.2. Squeezed states by changing the trap's frequency

If we consider no interaction with a laser, i.e., $\Omega = 0$, the Hamiltonian for the ion with an arbitrary (trap) frequency is simply [67]

$$H = \frac{1}{2} \left[p^2 + \omega^2(t) x^2 \right] \tag{227}$$

and we have seen that the transformation (212) produces the Hamiltonian

$$H = \frac{1}{2\rho^2(t)} \left(p^2 + x^2 \right) \tag{228}$$

which is in an integrable form. If we consider the vibrational motion state to be in a coherent state, $|\alpha\rangle$, then the evolved wave function reads

$$|\psi(t)\rangle = e^{-i\hat{I} \int_0^t \tilde{\omega}(\tau) d\tau} T_{SD}^\dagger(t) T_{SD}(0) |\alpha\rangle \tag{229}$$

where

$$\hat{I} = \frac{1}{2} \left[\frac{x^2}{\rho^2} + (\rho p - \dot{\rho} x)^2 \right] \tag{230}$$

is the so-called Lewis–Ermakov invariant. If we consider $\nu(t)$ to have the form as in Fig. 13, we can solve numerically the Ermakov equation, and obtain the auxiliary function, ρ, which we plot in Fig. 14; note that we will have a series of maximums and minimums. Because the transformation $T_{SD}^\dagger(t)$ depends on ρ, we can analyze from this figure the form in which the
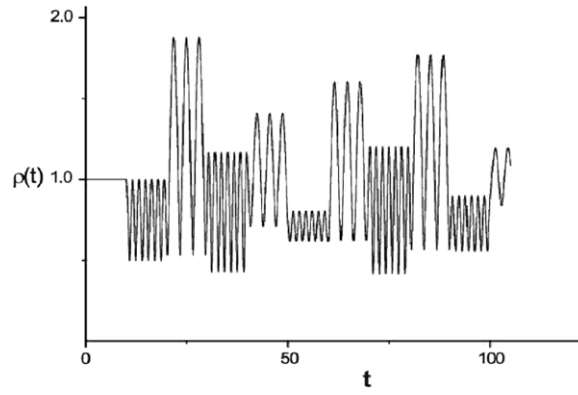
Fig. 14. Solution for the Ermakov equation for a time dependent frequency as shown in Fig. 13.

vibrational wave function is modified. Note from (212) that the second factor involves the derivative of ρ, which for the maximums and minimums is zero, making this exponential equal to one. Therefore, transformation (212) may be written for such times as

$$T_{SD}(t_M) = \exp\left\{\frac{i\ln\left[\rho(t_M)\sqrt{\nu_0}\right](xp + px)}{2}\right\};$$

(231)

i.e., a squeeze operator. Because $T_{SD}(0) = 1$ for this form of the time dependent frequency, if initially we start with a coherent state, squeezed states will be produced at times t_M.

7. Nonlinear coherent states and their modeling in photonic lattices

Nonlinear coherent states [68,69] may be generated in ion traps [14] and in this way realization of a quantum-mechanical counterpart of nonlinear optics has been achieved. For an appropriate laser-beam propagation geometry which affects only the dynamics in one vibrational mode of frequency ν, in the rotating-wave approximation, the Hamiltonian describing the effect of the Raman laser drive on the dynamics of the vibrational mode is given by Wallentowitz and Vogel [13]

$$H = \frac{\Omega}{2}\hat{g}_k(\hat{n})(i\eta a)^k + \text{H.C.},$$

(232)

with $\langle n|\hat{g}_k(\hat{n})|n\rangle = \frac{n!}{(n+k)!}L_n^{(k)}(\eta^2)e^{-\eta^2/2}$. If we consider the initial vibrational wave function to be in the vacuum state, after application of the evolution operator to this initial condition, a nonlinear coherent state is obtained. If we write the solution for the above Hamiltonian in the form

$$|\psi(t)\rangle = \sum_{n=0}^{\infty} u_n(t)|n\rangle,$$

(233)

and insert it into the Schrödinger equation, we obtain the following semi-infinite system of differential equations for the amplitudes $u_n(t)$ (for $k = 1$)

$$i\frac{du_0(t)}{dt} = \frac{\Omega}{2}f_1(1)u_1.$$

(234)

and

$$i\frac{du_n(t)}{dt} = \frac{\Omega}{2}\left(g_1(n)\sqrt{n}u_{n-1} + g_1(n+1)\sqrt{n+1}u_{n+1}\right), \quad n > 0$$

(235)

This system may be modeled in classical optics by light propagation in optical lattices as evanescently coupled waveguides have emerged as a promising candidate for the realization of an ideal, one-dimensional lattice with tunable hopping [70,71]. The system of differential equations given in (234) and (235) may be produced in a setup of waveguide arrays as the one in Fig. 15, thereby modeling the ion–laser Hamiltonian (232).
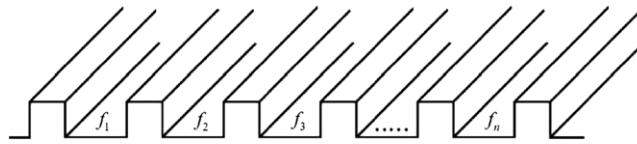
Fig. 15. A semi-infinite waveguide array where $f_k = g_1(k)\sqrt{k}$ is the corresponding coupling constant.

8. Conclusions

We have studied the ion–laser interaction, producing solutions that do not require too many approximations and allowing to reach ranges of parameters, such as Lamb-Dicke, detuning and intensity, not reached before. Exact linearization in the case of time dependent frequency has been shown by using Ermakov–Lewis invariant methods. In the case in which the frequency is considered constant, we have shown that it is possible to find exact eigenstates, access blue and red sidebands (a) in the low intensity regime without considering the rotating wave approximation and (b) in the on resonant case, by adjusting the intensity to half the trap's frequency, i.e., solely by intensity manipulation. We have also shown how a special class of nonclassical states, namely, *N00N* states may be produced in these systems and how the ion–laser interactions may be mimicked by a particular evanescent coupling of waveguides.

References

 [1] H.H. Kingdon, Phys. Rev. 21 (1923) 408.
 [2] F.M. Penning, Physica 4 (1937) 71.
 [3] W. Paul, Rev. Mod. Phys. 62 (1990) 531.
 [4] J.I. Cirac, P. Zoller, Phys. Rev. Lett. 74 (1995) 4091.
 [5] W.M. Itano, J.C. Bergquist, R.G. Hulet, D.J. Wineland, Physica Scripta T 22 (1988) 79.
 [6] D.J. Wineland, J.J. Bollinger, W.M. Itano, F.L. Moore, D.J. Heinzen, Phys. Rev. A 46 (1992) R6797.
 [7] J.J. Bollinger, J.D. Prestage, W.M. Itano, D.J. Wineland, Phys. Rev. Lett. 54 (1985) 1000.
 [8] H.F. Powell, M.A. van Eijkelenborg, W. Irvine, D.M. Segal, R.C. Thompson, J. Phys. B: At. Mol. Opt. Phys. 35 (2002) 205.
 [9] R.L. de Matos Filho, W. Vogel, Phys. Rev. A 58 (1998) R1661.
[10] D.M. Meekhol, C. Monroe, B.E. King, W.M. Itano, D.J. Wineland, Phys. Rev. Lett. 76 (1996) 1796.
[11] H. Moya-Cessa, S. Wallentowitz, W. Vogel, Phys. Rev. A 59 (1999) 2920.
[12] H. Moya-Cessa, S. Chávez-Cerda, W. Vogel, J. Mod. Optics 46 (1999) 1641.
[13] S. Wallentowitz, W. Vogel, Phys. Rev. A 55 (1997) 4438.
[14] S. Wallentowitz, W. Vogel, P.L. Knight, Phys. Rev. A 59 (1999) 531.
[15] Z. Kis, W. Vogel, L. Davidovich, Phys. Rev. 64 (2001) 033401.
[16] R.L. de Matos Filho, W. Vogel, Phys. Rev. Lett. 76 (1996) 608.
[17] R.L. de Matos Filho, W. Vogel, Phys. Rev. A 54 (1996) 4560.
[18] E.T. Jaynes, F.W. Cummings, Proc. IEEE 51 (1963) 89.
[19] H. Paul, Ann. Phys. (Leipzig) 11 (1963) 411.
[20] C.A. Blockley, D.F. Walls, H. Risken, Europhys. Lett. 17 (1992) 509.
[21] G.S. Agarwal, J. Mod. Opt. 34 (1987) 909;
     G.S. Agarwal, S. Arun Kumar, Phys. Rev. Lett. 67 (1991) 3665;
     G.S. Agarwal, J. von Zanthier, C. Skornia, H. Walther, Phys. Rev. A 65 (2002) 053826.
[22] B.W. Shore, P.L. Knight, J. Mod. Opt. 40 (1993) 1195.
[23] J.I. Cirac, R. Blatt, A.S. Parkins, P. Zoller, Phys. Rev. A 49 (1994) 1202.
[24] R.F. Bonner, J.E. Fulford, R.E. March, Int. J. Mass Spectrom. Ion Phys. 24 (1977) 255.
[25] P.J. Bardroff, C. Leichtle, G. Schrade, W.P. Schleich, Phys. Rev. Lett. 77 (1996) 2198.
[26] W.P. Schleich, Quantum Optics in Phase Space, Wiley-VCH, 2001.
[27] X. Zhu, D. Qi, J. Modern Opt. 39 (1992) 291.
[28] C.F. Roos, Ph.D. Thesis, Innsbruck, 2000.
[29] H. Dehmelt, Adv. At. Mol. Phys. 3 (1967) 53.
[30] H.R. Lewis, P.G.L. Leach, J. Math. Phys. 23 (1982) 165.
[31] M. Fernández-Guasti, H. Moya-Cessa, J. Phys. A 36 (2003) 2069.
[32] H. Moya-Cessa, M.F. Guasti, Phys. Lett. A 311 (2003) 1.
[33] H. Moya-Cessa, A. Vidiella-Barranco, J.A. Roversi, S. Dagoberto Freitas, S.M. Dutra, Phys. Rev. A 59 (3) (1999) 2518.
[34] R.J. Glauber, Phys. Rev. 131 (1963) 2766.
[35] D. Jonathan, M.B. Plenio, P.L. Knight, Phys. Rev. A 62 (2000) 042307.
[36] F.A.M. de Oliveira, M.S. Kim, P.L. Knight, V. Buzek, Phys. Rev. A 41 (1990) 2645.
[37] J. Evers, C.H. Keitel, Europhys. Lett. 68 (3) (2004) 370.
[38] D. Leibfried, R. Blatt, C. Monroe, D. Wineland, Rev. Mod. Phys. 75 (2003) 281.
[39] D.J. Wineland, C. Monroe, W.M. Itano, D. Leibfried, B.E. King, D.M. Meekhof, J. Res. Natl. Inst. Stand. Technol. 103 (1998) 259.
[40] D. Leibfried, D.M. Meekhof, B.E. King, C. Monroe, W.M. Itano, D.J. Wineland, Phys. Rev. Lett. 77 (1996) 4281.
[41] M. Sasura, V. Buzek, J. Modern Opt. 49 (2002) 1593.
[42] H. Moya-Cessa, P. Tombesi, Phys. Rev. A 61 (2000) 025401.
[43] H. Moya-Cessa, D. Jonathan, P.L. Knight, J. Mod. Optics 50 (2003) 265.
[44] J.M. Vargas-Martínez, E.A. Martí-Panameo, H. Moya-Cessa, Rev. Mex. Fís 55 E (2009) 176.
[45] A. Zúñiga-Segundo, J.M. Vargas-Martínez, R. Juárez-Amaro, H. Moya-Cessa, Annalen der Physik (2012).
[46] J.G. Peixoto de Faria, M.C. Nemes, Phys. Rev. A 59 (1999) 3918.
[47] A. Klimov, L.L. Sánchez-Soto, Phys. Rev. A 61 (2000) 063802.
[48] W.H. Louisell, Quantum Statistical Properties of Radiation, Wiley, NewYork, 1973.
[49] D.T. Pegg, S.M. Barnett, Europhys. Lett. 6 (1988) 483;
     D.T. Pegg, S.M. Barnett, Phys. Rev. A 39 (1989) 1665.

[50] M. Abramowitz, I.A. Stegun, Handbook of Mathematical Functions With Formulas, Graphs, and Mathematical Tables. National Bureau of Standards. Applied Mathematics Series.
[51] I.S. Gradshteyn, I.M. Ryzhik, Table of Integrals, Series and Products, Academic Press, Inc., 1980.
[52] L. Mandel, Opt. Lett. 4 (1979) 205.
[53] E. Schrödinger, Naturwissenschaften 23 (1935) 807. 823, 844.
[54] B. Yurke, D. Stoler, Phys. Rev. Lett. 57 (1986) 13.
[55] R. Loudon, P.L. Knight, J. Modern Opt. 34 (1987) 709.
[56] I. Afek, O. Ambar, Y. Silberberg, Science 328 (2010) 879.
[57] J.P. Dowling, Contemp. Phys. 49 (2008) 125.
[58] F. Wolfgramm, A. Cere, M.W. Mitchell, J. Opt. Soc. Amer. 27 (6) (2010) A25–A29.
[59] Y. Bromberg, Y. Lahini, Y. Silberberg, Phys. Rev. Lett. 105 (2010) 263604.
[60] D. Rodríguez-Méndez, H. Moya-Cessa, Opt. Commun. 284 (2011) 3345.
[61] S.G. Zheng, Phys. Rev. A 63 (2000) 015801.
[62] L. Susskind, J. Glogower, Physics 1 (1964) 49.
[63] B. Sherman, G. Kurizki, Phys. Rev. A 45 (1992) R7674;
     B.M. Garraway, B. Sherman, H. Moya-Cessa, P.L. Knight, G. Kurizki, Phys. Rev. A 49 (1994) 535.
[64] K. Vogel, V.M. Akulin, W.P. Schleich, Phys. Rev. Lett. 71 (1993) 1816.
[65] G. Schrade, V.I. Man'ko, W.P. Schleich, R.J. Glauber, Quantum Semiclass. Opt. 7 (1995) 307.
[66] G. Schrade, P.J. Bardroff, R.J. Glauber, C. Leichtle, V. Yakovlev, W.P. Schleich, Appl. Phys. B 64 (1997) 181.
[67] V.V. Dodonov, V.I. Man'ko, Phys. Rev. A 20 (1979) 550.
[68] V.I. Man'ko, G. Marmo, F. Zaccaria, E.C.G. Sudarshan, Physica Scripta 55 (1997) 528.
[69] A. Mikhalychev, D. Mogilevtsev, S. Kilin, J. Phys. A 44 (2011) 325307.
[70] A. Perez-Leija, H. Moya-Cessa, A. Szameit, D.N. Christodoulides, Opt. Lett. 35 (14) (2010) 2409–2411.
[71] R. Keil, A. Perez-Leija, F. Dreisow, M. Heinrich, H. Moya-Cessa, S. Nolte, D.N. Christodoulides, A. Szameit, Phys. Rev. Lett. 107 (2011) 103601.